Master's thesis

NTNU
Norwegian University of Science and Technology
Faculty of Information Technology and Electrical Engineering
Department of Electric Power Engineering

Marius Strand

Contact Degradation in Air Load Break Switches by Making Operation under Short Circuit Condition

Master's thesis in Energy and Environmental Engineering
Supervisor: Kaveh Niayesh
Co-supervisor: Naghme Dorraki
June 2021

NTNU
Norwegian University of
Science and Technology

Marius Strand

Contact Degradation in Air Load Break Switches by Making Operation under Short Circuit Condition

Master's thesis in Energy and Environmental Engineering
Supervisor: Kaveh Niayesh
Co-supervisor: Naghme Dorraki
June 2021

Norwegian University of Science and Technology
Faculty of Information Technology and Electrical Engineering
Department of Electric Power Engineering

NTNU
Kunnskap for en bedre verden

Abstract

The operation of electrical switchgear is essential for a functional and reliable power grid. In the distribution network, load break switches can be utilized as a cost-competitive alternative to circuit breakers. However, this raises other issues. Load break switches are required to perform several making operations where a high short circuit current passes through. During making operation, an arc is established when the contacts are closing. This is due to a dielectric breakdown. The arc leads to high energy dissipation between the contacts, which results in contact erosion and eventually welding. This is highly undesirable and may affect the future functionality of the switch.

This thesis investigates contact degradation in load break switches during making operation under short circuit conditions. By utilizing a synthetic test setup consisting of an HVDC source and a high current transformer, the contacts have been exposed to stresses during making operation. Four different test cases have been applied to improve the understanding of this process. The energy dissipation depends on the arc voltage, the short circuit current, and the arcing time. All these parameters have been recorded during the experimental testing. Additionally, the effect of the main contacts has been examined.

Pre-strike arc energy and mass loss measurements have been performed for each test. The results clearly show that higher short circuit currents will increase the arc erosion on the arcing contacts. Additionally, an increase in closing velocity will decrease the contact degradation. The mass loss was highest for the worst-case scenario with a closing velocity of 2.9 m/s and a short circuit current of 20kA. Welding was achieved after seven and four tests, with and without main contacts, respectively. This clearly shows that the main contacts are important during making operation and will extend the lifetime of the switch. The results also show that welding is dependent on both arc energy and the degree of contact erosion that gradually occurs by repeated making operations.

Sammendrag

Koblingsutstyr er sentralt for et velfungerende og pålitelig strømnett. I distribusjonsnettet kan lastbrytere benyttes som et konkurransedyktig alternativ til effektbrytere. Dette kan derimot føre til andre utfordringer. Det kreves at lastbrytere kan utføre flere lukkeoperasjoner hvor høye kortslutningsstrømmer flyter gjennom bryteren. Når bryteren lukkes, vil en lysbue dannes som følge av et gjennomslag. Når lysbuen brenner mellom kontaktene fører dette til høye temperaturer som kan skade lysbuekontaktene. Potensielt kan dette føre til at lysbuekontaktene sveises sammen og at lastbryteren ikke fungerer slik den skal neste gang den skal bryte strømmen.

Denne masteroppgaven undersøker hvordan lysbuekontaktene i en lastbryter blir påvirket under lukkeoperasjoner. Det er benyttet et syntetisk testoppsett bestående av en HVDC spenningskilde og en transformator for å utsette lysbuekontaktene for påkjenninger under lukking. Fire ulike testkonfigurasjoner med ulik lukkehastighet og kortslutningsstrøm er benyttet. Lukkehastighet, kortslutningsstrøm og lysbuespenning er parametre som påvirker energien i lysbuen under lukking. For å undersøke hvordan denne energien påvirker lysbuekontaktene er de nevnte parameterne målt. Det er utført forsøk både med og uten hovedkontakt. Dette er for å undersøke effekten av hovedkontakten, og om bryterens levetid er avhengig av den.

For hver test er det blitt utført målinger av massetap og lysbueenergi. Resultatene viser at høyere kortslutningsstrømmer fører til mer erosjon på lysbuekontaktene. En økt lukkehastighet vil føre til mindre skade på kontaktene. Massetapet var høyest for testkonfigurasjonen med lavest lukkehastighet og høyest kortslutningsstrøm. Kontaktene ble sveiset etter syv tester med hovedkontakt, og etter fire tester uten hovedkontakt. Dette viser tydelig at hovedkontaktene er viktig for å forlenge levetiden til lastbryteren. Resultatene har vist at sveising av kontaktene er avhengig av både lysbueenergi og graden av erosjon fra tidligere lukkeoperasjoner.

Preface

This thesis is submitted to the Department of Electric Power Engineering at the Norwegian University of Science and Technology (NTNU), Trondheim, fulfilling the requirements for the degree of Master of Science. It is a continuation of my specialization report, and the aim is to improve the understanding of contact erosion during making operation for medium voltage load break switches.

I would like to thank my supervisor, Professor Kaveh Niayesh at NTNU, for his support during this work. I highly appreciate that you have always taken the time to answer my questions.

I am grateful to my co-supervisor, Ph.D. Candidate Naghme Dorraki at NTNU. She has been my primary source of guidance during the laboratory work. I am thankful for all feedback you have given me and the discussions we have had during this work.

Trondheim, June 2021

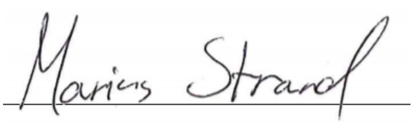

Marius Strand

Contents

List of Tables

List of Figures

Abbrevations

CB	Circuit breaker
CuW	Copper-tungsten
HV	High voltage
HVDC	High voltage direct current
IEC	International Electrotechnical Commission
LBS	Load break switch
MV	Medium voltage
SA	Surge Arrester
$\mathbf{SF_6}$	Sulfur hexafluoride
TVS	Triggered vacuum switch

Chapter 1

Introduction

1.1 Background

The demand for energy is increasing, and the electric power grid faces new challenges. In a well-functioning grid, power switching components have an essential role. Switchgear is used for making and interrupting current. This enables control of the power flow in case of any faults or planned maintenance. The primary task of any switching device is to open or close connections. Therefore, it should be able to act as both an insulator and a conductor.

Switchgear is present throughout the grid. Depending on factors like voltage level and current amplitude, the ratings and requirements vary. In the distribution network, the voltage level is in the range of 6 - 36 kV with currents up to 1 kA. Load break switches (LBSs) can be utilized as a cost-efficient alternative to the more expensive circuit breaker. The LBS is a switch that can conduct, interrupt and make currents up to its rated load current. To interrupt larger fault currents, the LBS is often placed in series with fuses.

The motivation is to develop an LBS that does not utilize sulfur hexafluoride (SF_6) as interrupting medium. SF_6 is a gas with a high global warming potential. It is desirable to replace this gas with air or other non-greenhouse gases. SF_6 is frequently used due to its superior properties as interrupting medium. By replacing this gas, other issues are raised regarding switchgear design. A lower dielectric strength results in a longer presence of the arc during making operation. Consequently, the energy dissipation will increase.

Hence, the switch is exposed to higher thermal stresses that will lead to contact degradation. Energy dissipation is dependent on pre-strike voltage, short circuit current, and the arcing time or the closing velocity. By adjusting these parameters, it is possible to obtain less thermal stresses. Therefore, it is desirable to investigate how each of those parameters will affect contact degradation. Contact degradation may lead to contact welding, and consequently, failure in the next switchgear operation.

1.2 Research Objectives

The work carried out in this thesis is an experimental study on how different parameters will affect contact degradation during making operation of medium voltage (MV) LBSs. It is a continuation of the work performed in [10]. This thesis aims to provide a basis for better understanding LBS design parameters and contact material to prevent erosion and welding when high fault currents pass through switchgear during making operation. This will provide an insight into how erosion will affect the performance and lifetime of an LBS. The test object is a horizontal moving contact released by a solenoid electromagnet. A synthetic test setup has been utilized to supply pre-strike voltage and short circuit currents.

1.3 Structure of Thesis

The structure of this report is as follows: Firstly, a theory chapter is presented. This theory forms the basis to understand the making operation and erosion related to the arc. Additionally, a literature study is included. The experimental method is described in Chapter 3. This provides detailed information about the test object, the parameters, and how the experimental work is performed. In Chapter 4, the results from the experimental work are presented. Throughout this chapter, the results are discussed. Conclusions based on analysis and the discussion are found in Chapter 5. The final chapter contains suggestions for further work.

Chapter 2

Theory

In this chapter, the theoretical basis for current making and contact degradation is presented. Additionally, a literature study has been performed. This work was carried out in the specialization project [10] preceding this thesis. However, some modifications have been made.

2.1 Switchgear

Switchgear are components used to control, protect and isolate parts of the electric network or equipment. It is used to de-energize parts of the network if there are any planned services and to clear faults. If a fault occurs, switches are used to change the power flow to sustain the power supply to as many consumers as possible.

The following requirements apply to any type of switchgear [3]:

- Behave as an electrical conductor in closed position. The current should be able to flow through the switch without any significant voltage drop.
- Behave as an electrical insulator in open position. It should withstand any voltages that may be applied.
- Be able to break any current lower than the maximum rated breaking current.
- Be able to close at any time without welding the contacts.

Depending on location in the grid and under what conditions the switch will operate, there is a vast selection of switchgear. The goal is to find the optimal solution regarding electrical characteristics and cost. Switching components can be categorized into four types depending on characteristics and performance [3]:

- Disconnector Switch
- Earthing Switch
- Circuit Breaker (CB)
- Load Break Switch (LBS)

The disconnector switch is used to open energized circuits but cannot interrupt any load or short circuit currents. The earthing switch connects parts of the grid to ground. It can carry high currents but not interrupt any currents. The CB should be able to interrupt all types of currents and has the most demanding tasks. The LBS is able to interrupt currents up to the rated current and is typically used in the distribution grid. It can be combined with the properties of a disconnector switch, resulting in a switch-disconnector. It is often placed in series with fuses that can interrupt larger fault currents. Compared to a CB, an LBS is a more affordable alternative.

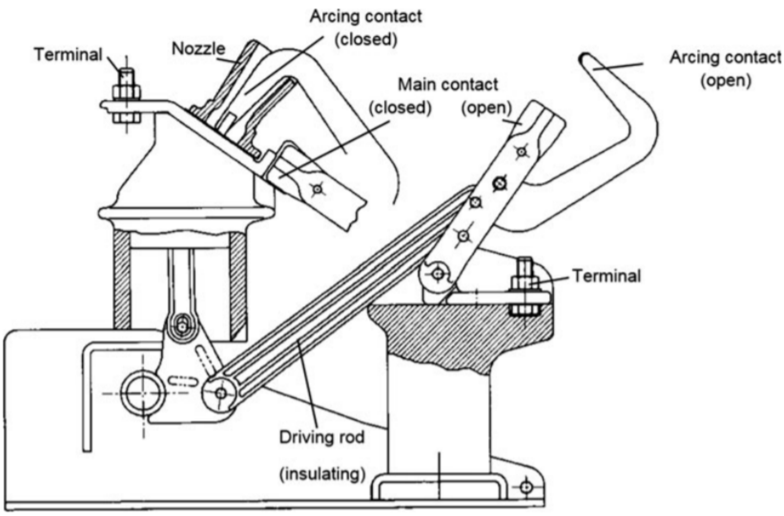

Figure 2.1: A load break switch in both open and closed position [3].

In Figure 2.1, an LBS is illustrated in both open and closed position [3]. It consists of two pairs of contacts, the arcing contacts and the main contacts.

2.1.1 Stresses on Switchgear

Once a switch is installed and in operation, it will be exposed to different types of stresses. Stresses may have an impact on the functions and lifetime of switches. There are three main types of stresses regarding switchgear [3]:

- Mechanical stresses
- Dielectric stresses
- Thermal stresses

Mechanical stresses in switchgear are present during operation as a consequence of fast-moving parts. In addition, increased internal pressure during the interruption process causes mechanical stresses. It also occurs during a short circuit when high forces are affecting the equipment.

When the switch is in the open position, it should act as an insulator. Therefore the dielectric strength must be high. If a sufficiently high voltage is applied to a material or medium, it will lead to discharges. If the discharge bridges the insulation, a dielectric breakdown will occur [11]. With a higher dielectric strength, a higher voltage applied is required to cause a breakdown. In the power system, there are temporary overvoltages and overvoltages caused by switching and lightning [12]. These overvoltages will expose the switch to dielectric stresses.

In the grid, there will always be power losses resulting in heating of equipment. Increased temperature can cause the material to deteriorate. Short circuit currents can cause a higher temperature rise, but this will subside after a short time. Furthermore, parts of the switch will experience thermal stresses due to the electric arc during switchgear operation. High temperatures in the arc may lead to erosion, welding or vaporization of the contact surfaces.

2.2 Making of Short Circuit Current

Any type of switchgear has two main operations in the power grid, either opening or closing. In the open position, the switch should be able to close, also referred to as current making. In closed position, the current will flow through the switch. The making operation happens fast, a question of milliseconds.

This operation starts when the switch gets a signal to close. Then the moving contact is released and travels towards the stationary contact. Once the electric field exceeds the dielectric strength of the insulating medium, an electric arc will be formed. In this arc, the current will flow through even before the solid contacts are in touch. This is called a pre-strike and will occur if the applied voltage to the switch is sufficiently high or the gap distance is correspondingly short [3]. When a current flows through the arc, energy is dissipated. This leads to an increase in temperature in the arc, and some of this thermal energy will be absorbed by the contacts. The dissipated energy in the arc during making can be calculated by Equation 2.1 [3].

$$E_{dissipation} = \int_{t_{breakdown}}^{t_{touch}} i_{sc}(t) \cdot u_{arc}(t) dt \tag{2.1}$$

i_{sc} is the short circuit current flowing in the arc. u_{arc} is the arc voltage. $t_{breakdown}$ is when the dielectric breakdown in the gap occurs, while t_{touch} is the time when the contacts are in touch. The time limits are illustrated in Figure 2.2 [3].

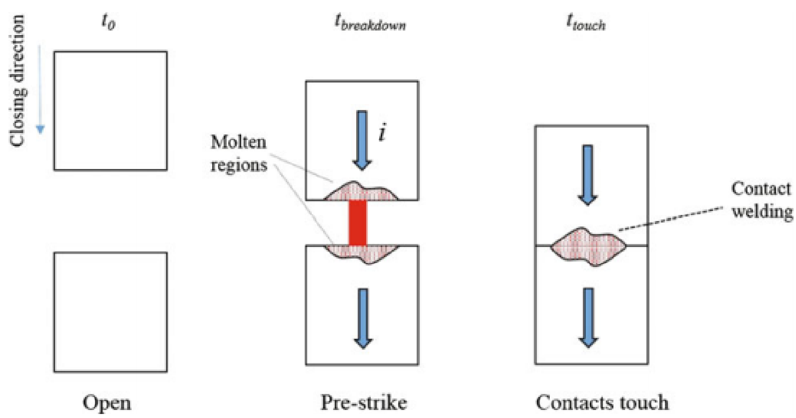

Figure 2.2: Illustration of welding during making operation [3].

As seen in Equation 2.1, energy dissipation is time-dependent. As a result of this, it is desirable to minimize the arcing time. In Figure 2.2, it can be seen that there are molten regions on the contacts. This is due to high temperatures in the arc. Making with molten contacts can lead to contact welding. This is highly undesirable and may cause problems during the next switchgear operation. If the weld force is greater than the mechanical force in the switch, it will not be able to open. Tepper et al. [5] investigated the erosion of arcing contacts in a circuit breaker. The aim was to provide a method to predict contact erosion of HVCB. They discovered that the specific erosion would be increased with the amplitude of the arcing current and the time of the arc.

Regarding failure in the switchgear, Jansen et al. [13] state that the mechanical operating mechanism is responsible for most failures in CBs. Razi-Kazemi et al. [4] investigated a failure prediction approach for spring-type HVCBs focusing on travel curves. The travel curve is a tool to monitor contact displacement as a function of time. In Figure 2.3 an example is shown with a normal and a faulty switch [4]. It can be seen that the normal one bounces slightly before stabilizing. The faulty switch is not able to close and goes back to open position. Erosion and welding due to bounce arcs are some of the stresses the contact material is exposed to during making operation [14].

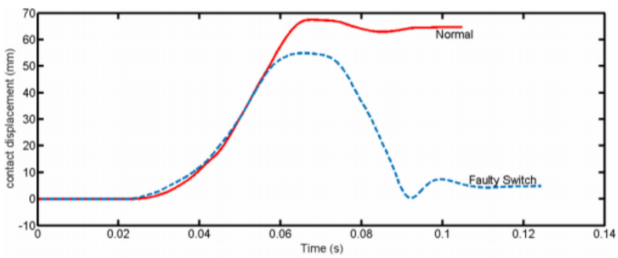

Figure 2.3: Travel curve profile during making operation of a normal and a faulty switch [4].

Kharin and Nouri [15] investigated the dynamics of arc phenomena at making in vacuum CBs. They found that contact bouncing depends on five force components. These are spring force, elastic-plastic force at compression, electromagnetic repulsion force, force of metallic vapor, and welding force. The electromagnetic repulsion force will counteract the closing forces. Consequently, the closing movement may stop before the contacts are sufficiently in touch. This phenomenon also applies to gas CBs and LBSs.

2.2.1 Current Commutation

Switchgear usually consists of two pairs of contacts, the main contacts and the arcing contacts. In the closed position, the current flows through the main contacts. The arcing contacts are where the arc burns, and current interruption and making occur [3]. During the making process, the arc establishes between the arcing contacts when the breakdown takes place. In the fully closed position, the main contacts will carry the load current. The contact pairs are illustrated in Figure 2.4. It can be seen that the arcing contacts will close first. Thereafter, the main contacts will close.

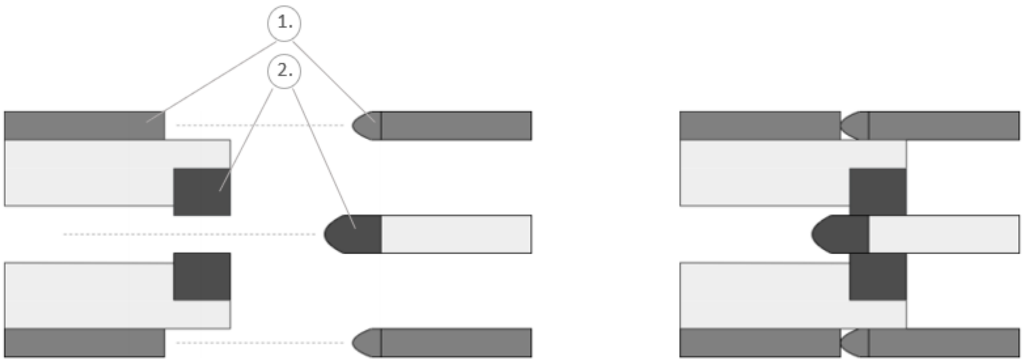

Figure 2.4: Illustration of 1. main contacts and 2. arcing contacts in open and closed position.

During the operation of switchgear, the current commutation phase between main and arcing contacts is important. This operation can be explained by the equivalent circuit in Figure 2.5 [3].

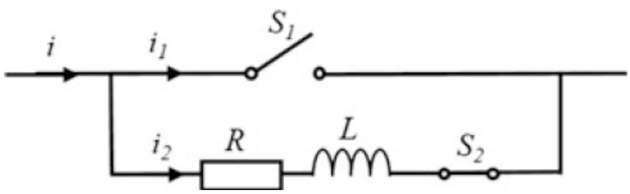

Figure 2.5: Equivalent circuit of contacts during current commutation [3].

Here S_1 is the main contacts and S_2 is the arcing contacts. R is the resistance in the arcing contacts, while L is the total inductance of the loop between the two contacts. During making operation S_2 will close first and protect the main contacts against stresses due to the arc. Later, S_1 will close and almost all of the current will flow through that branch due to a much smaller resistance compared to the arcing contacts [3].

2.3 Contact Material

As previously mentioned, the contact surfaces are exposed to high forces and stresses during making operation. To withstand these impacts, material selection is important. There are several materials with different properties that are used in the electrical system. In cables and lines, copper and aluminum are widely used in the electric grid. Silver has the highest electrical conductivity, and non-arcing electrical contacts are usually made of a silver-based alloy [16]. Silver is expensive, and therefore it is preferable to use other materials. During making, temperatures can reach levels that will damage materials that are widely used. An alloy can be used to reduce degradation and the likelihood of welding. This alloy should consist of materials with good electrical and thermal conductivity. Additionally, a high melting and boiling point is important to withstand the thermal stresses. In Table 2.1, the properties mentioned for copper, aluminum, silver and tungsten are shown.

Table 2.1: A selection of the properties of copper, aluminum, silver and tungsten [1].

	Copper (Cu)	**Aluminum (Al)**	**Silver (Ag)**	**Tungsten (W)**
Electrical Conductivity	$5.96 \cdot 10^7/\Omega m$	$3.5 \cdot 10^7/\Omega m$	$6.3 \cdot 10^7/\Omega m$	$1.79 \cdot 10^7/\Omega m$
Thermal Conductivity	401 W/m·K	237 W/m·K	429 W/m·K	173 W/m·K
Melting Point	1358 K	934 K	1235 K	3683 K
Boiling Point	2835 K	2740 K	2485 K	5933 K

Mützel et al. [17] studied the effect of material composition on welding. They investigated different silver metal oxides and their behavior during making operation. Their result indicates that the weld break force may be decreased by increasing total metal oxide content. It is also important to use materials that have a sufficiently high melting point. Regarding arc erosion, materials with a low melting point are considered as poor [18].

2.4 Contact Erosion

Due to the energy dissipation during making operation, contact erosion will occur. This is a result of high temperatures in the switching arc. According to Tepper [5], the temperature in the arc is somewhere in between 20 000 - 30 000 K. Further, the temperature at the contact surface rises to about 5000 - 6000 K. Shea [2] defines contact erosion as a change in the mass, either loss or gain. High temperatures result in melting, vaporization and ablation of the contact material. This results in degradation or restructuring of the contact surfaces. This is illustrated in Figure 2.6 [2]. T_M is the molten area, and T_B is the boiling area of the contact.

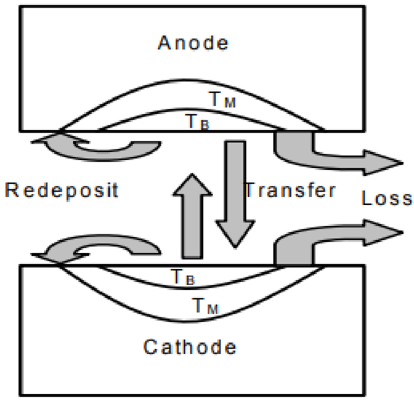

Figure 2.6: Example of contact erosion and mass changes in anode and cathode. T_M is the molten zone, and T_B is the boiling zone [2].

There are several factors that will affect contact erosion. They can be either electrical, contact or device parameters. These factors influencing contact erosion during high-current switching are summarized in Table 2.2 [2].

Table 2.2: Factors affecting contact erosion (Reproduced after [2]).

Parameters	Factors
Electrical	Arc Energy, Current, Phase Angle, Arcing Time, Charge
Contact	Material Properties, Processing, Size and Shape, Number of Phases
Device	Opening Speed, Arc Running, Open Gap Length, Arc Quenching, Heat Sinking, Gassing Material, Venting, Arc Shape, Make or Break

Wilson [18] investigated high-current arc erosion and found that contact erosion is increased at smaller gaps. This resulted from increased gas pressure and speed of vapor due to the small space between the contacts. Further, it was found that erosion mechanisms related to low current could not be used to determine erosion caused by high current. It was concluded that the primary mechanism of erosion is the vaporization of contact material. The secondary is that the vaporized material forces droplets of the liquid contact surface away.

Tepper et al. [5] looked into the erosion of copper-tungsten (CuW) contacts in HVCB during current interruption. Due to high arc temperatures, copper will be vaporized, and tungsten will be liquefied. As a result, the contact surface will be a layered structure as seen in Figure 2.7 [5]. This layered structure was confirmed by the use of a scanning electron microscope (SEM).

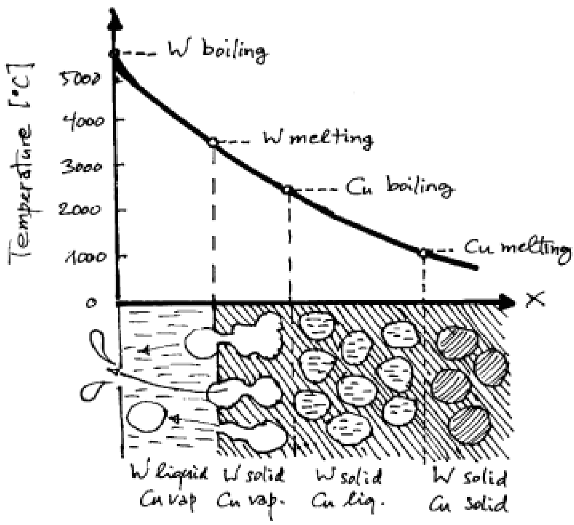

Figure 2.7: The layered structure of the contact surface after being exposed to heating [5].

After an operation, the temperature goes back to normal and the thermal effects can be observed. After cooling, there is a tungsten skeleton with re-solidified tungsten at the surface. This process will go on for the next arcing and gradually deteriorate the switch and shorten the lifetime. An illustration of this re-solidified CuW contact is shown in Figure 2.8 [6].

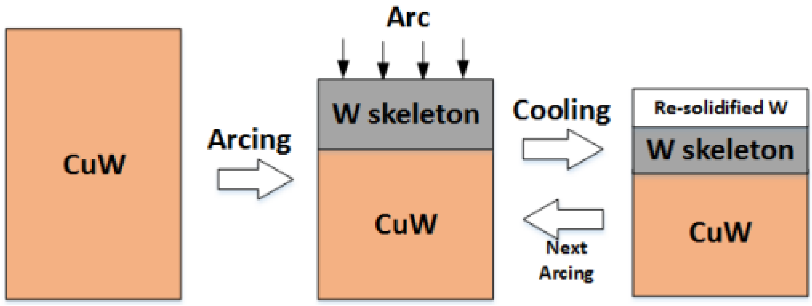

Figure 2.8: Development of the CuW contact during arcing [6].

2.4.1 Contact Welding

An undesired consequence of erosion is contact welding. According to Slade [14], all contacts weld to a certain extent. It can occur if high currents are flowing through closed contact or during current making, either from the pre-strike arc or bouncing arcs. The real problem occurs if the weld force exceeds the mechanical force that opens the switch. As a result, the switch will not be able to operate as it should. Kharin et al. [15] conclude that the welding probability can be estimated by the relation of closing velocity and current amplitude. Hotta et al. [16] state that the weld force increases for higher arc currents and arc durations. In addition, they found that the melted zone of the contact will increase with an increase in the arc energy. These studies have investigated contact welding in vacuum CBs and low voltage switches, respectively.

In previous work presented in [19], the impact of the pre-strike voltage has been shown. The LBS failed to re-open after three tests at the highest voltage level. In addition, the mass loss was increased at the higher voltage level. This shows that all three parameters that affect energy dissipation play an essential role in contact welding.

The extent of welding can be determined by the weld force. The weld force F_W is given by:

$$F_W = \Gamma A_W \tag{2.2}$$

Γ is the tensile strength of the contact material, and A_W is the welded area. The tensile strength varies for different materials. In Table 2.3, a range of the tensile strength for a selection of materials is shown.

Table 2.3: Tensile strength of copper, aluminum, silver and tungsten.

Metal	Tensile Strength ($10^8 Nm^{-2}$)
Cu wire	2.8 - 4.6
Al wire	0.47 - 0.9
Ag wire	2.3 - 3.5
W wire	15 - 35

2.5 Interrupting Medium

Interrupting medium is a medium that is enclosed in the interrupting chamber where the arc is burning. This is usually a gas, but oil and vacuum are also utilized for this purpose. To act as a perfect interrupting medium, there are some requirements regarding the properties of the medium. The most important with respect to arc interruption are listed below [20]:

- High dielectric strength
- High thermal conductivity
- Fast gas recovery
- Self-healing/dielectric integrity

SF_6 dominates as interrupting medium at voltage levels above 100 kV. Furthermore, it is also extensively used in the distribution network operating at medium voltages [3]. This is due to its good insulation and arc quenching properties. It is an electronegative gas that will absorb free electrons, which results in slow negative ions. This makes it more challenging for an electron avalanche to be created. Consequently, a higher voltage is required to cause a breakdown. In Figure 2.9, SF_6 is compared to vacuum and air regarding their dielectric strength [3].

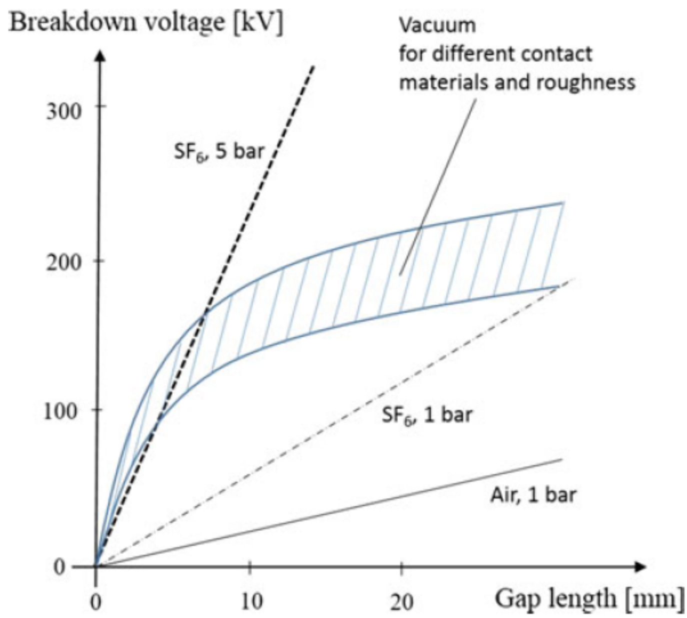

Figure 2.9: The dielectric strength for vacuum, SF_6 and air for different gap lengths in a homogeneous electric field [3].

The properties of SF_6 result in compact and reliable components. However, there is a significant drawback regarding the environmental impact of the gas. As stated by Myhre et al. [21], the global warming potential of SF_6 is 23.500 times greater than CO_2. Additionally, the process of the natural decomposition of the gas is very slow.

Therefore, it is preferable to utilize other gases in switchgear. Air is an environmentally friendly alternative but raises other challenges regarding the operation of switchgear. This is due to a lower dielectric strength that varies with temperature and pressure [11]. As a result, the pre-strike during making will occur earlier. Hence, there will be a higher energy dissipation and an increased probability of erosion and welding. This impacts the design of air-based switchgear. It is a challenging task to design it comparatively compact [22]. Stoller et al. [23] investigated the performance of CO_2 as an arc interruption medium in gas circuit breakers. Their findings indicate that, for a fixed pressure, CO_2 performs better than air regarding arc interruption performance. The conclusion was that SF_6 is still the better option. Kosse et al. [24] studied other SF_6 alternatives in different mixtures of CO_2. CO_2 was mixed with the fluor compounds fluoronitrile and fluoroketone. Both performed better compared to SF_6 regarding low environmental impact. However, the performance of the alternatives regarding technical performance was around 80% compared to SF_6. AirPlus is another alternative as interrupting medium that matches SF_6 when it comes to the required properties. It is a fluoroketone-based gas mixture that also consists of nitrogen and oxygen for MV gas-insulated switchgear. It decomposes rapidly compared to SF_6, and the carbon footprint is lower than CO_2 [25].

2.6 Test Methods

In order to assess switchgear under controlled conditions, a laboratory test setup is needed. These kinds of tests are used to develop and modify switches. It is possible to investigate how new materials will perform and how modifications regarding parameters will affect switchgear operation. To perform a test, there are two possible methods. According to the International Electrotechnical Commission (IEC) standard for high-voltage switchgear and controlgear 62271-101 these are [7]:

- Direct testing
- Synthetic testing

Direct testing is a test where one single power source supplies both voltage and current. In cases where both high voltage and high current are required, a powerful power supply is needed. Therefore, testing of switchgear in MV and HV levels is close to unattainable by direct testing. However, that issue can be solved by utilizing a synthetic test setup. In a synthetic test, there are two separate sources. High voltage and high current do not appear simultaneously during the test and can therefore be supplied by two different sources [3]. During a making test, the high voltage period will happen first. After the arc is established and the contacts are closing, the high current (simulating the short circuit current) will flow through the switch. This test requires synchronization, so the HV and high current occur in the right order.

During a synthetic test there are three intervals [7]:

- High-voltage interval
- Pre-arcing interval
- Latching interval

The high-voltage interval is the time between the start of the test and until breakdown occurs. The test object is in the open position at t_0 and then starting to close. The pre-arcing interval is the period from when the breakdown occurs to when the contacts physically touch. Finally, the latching interval is the time from the contacts first touch to the moment where the main contacts are in the fully closed position.

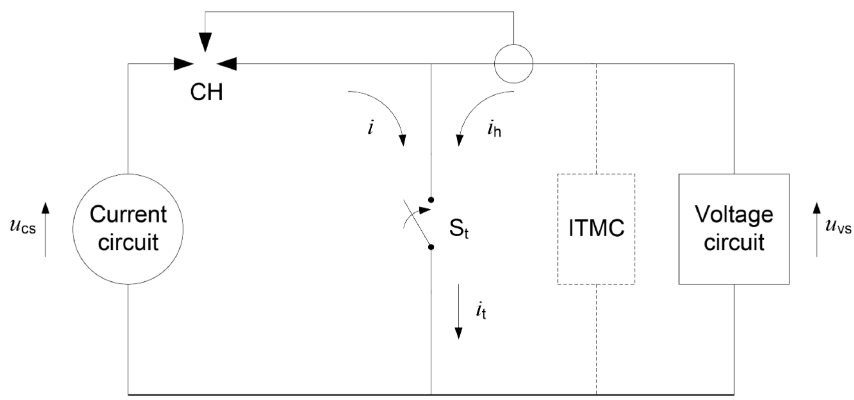

Figure 2.10: The standard setup of a synthetic making circuit for single-phase tests [7].

In Figure 2.10, the standard setup for a single-phase making test according to IEC is shown [7]. There are two circuits, the high current on the left side and the high voltage on the right side. ITMC is short for initial transient making current, and S_t is the test object. CH is the making device, here a triggered spark gap.

Chapter 3

Experimental Method

In this chapter, the experimental method is described. A synthetic test circuit with a spring-type switch has been utilized. The different parameters related to arc dissipation and the applied values are presented. All the experiments in this work are performed in surrounding air at atmospheric pressure. The setup is the same that was applied in [10]. Although, there have been some changes regarding the test object and which parameters are adjusted.

3.1 Experimental Setup

The experimental setup can be divided into three main parts:

- High voltage circuit
- High current circuit
- Synchronization

A synthetic test method is utilized. The test circuit is shown in Figure 3.1, including a high current circuit and high voltage circuit. The only component present in both circuits is the test object. The test circuit is the same that was used in [8].

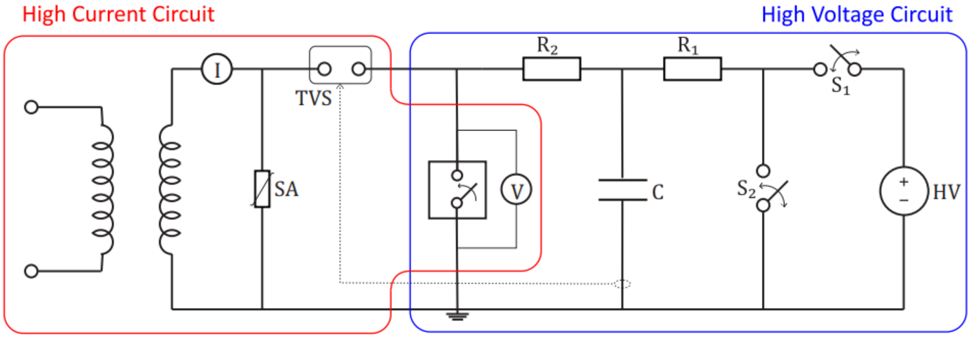

Figure 3.1: Schematic of the test circuit. High current circuit (red) and high voltage circuit (blue) [8].

3.1.1 High Voltage Circuit

The high voltage circuit consists of a high voltage direct current (HVDC) source, two switches, two resistances and a capacitor. The values related to the impedance in the circuit can be seen in Table 3.1. The high voltage circuit provides the voltage that causes the pre-strike.

Table 3.1: Component values of the HV circuit.

Component	Value
R_1	200 Ω
R_2	75 Ω
C	0.1 μF

There is additionally a Rogowski coil (grey dotted circle) to measure current flow. The function is related to the high current circuit and will be described in Section 3.1.2. S_2 is a switch that connects the source to ground. This is to avoid undesirable charging of the capacitor. When running a test, S_2 is in open position. S_1 connects the power source to the capacitor. Once the capacitor is fully charged, S_1 is opened before the test object is closing. Consequently, the pre-strike over the test object will occur.

3.1.2 High Current Circuit

The high current circuit consists of a high current transformer, a surge arrester (SA) and a triggered vacuum switch (TVS). The high current transformer supplies the short circuit current with a frequency of 50 Hz that will pass through the test object. The purpose of a SA is to protect against any transient overvoltages caused by dielectric breakdown during the switching operation [12]. If any overvoltages occur, the SA will connect to ground and protect the transformer. The TVS will connect the transformer to the test object. The Rogowski coil triggers the TVS. When the pre-strike occurs and current passes through the Rogowski coil, a signal is sent to an optical pulse shaper and further on to the trigger driver. The trigger driver then sends a signal to the TVS to close. Consequently, the current from the transformer will flow through the pre-strike arc over the test object.

3.1.3 Synchronization

In a synthetic test, synchronization is essential. The time of breakdown from the high voltage circuit needs to be matched with a current zero of the transformer current. Then, a full half-cycle of current can pass through the test object during making operation. In this experimental series, where the effects of arcing are investigated, one half-cycle is sufficient. With a current frequency of 50 Hz, the resulting half-period is equal to 10 ms.

In Figures 3.2(a) and 3.2(b), an HV breakdown test and the output current of the transformer is shown. In this example, the voltage and current are approximately 18 kV and 15 kA, respectively. The synchronization is performed by the time setting of the release of the moving contact. The accuracy of the synchronization system is $\pm$ 1 ms.

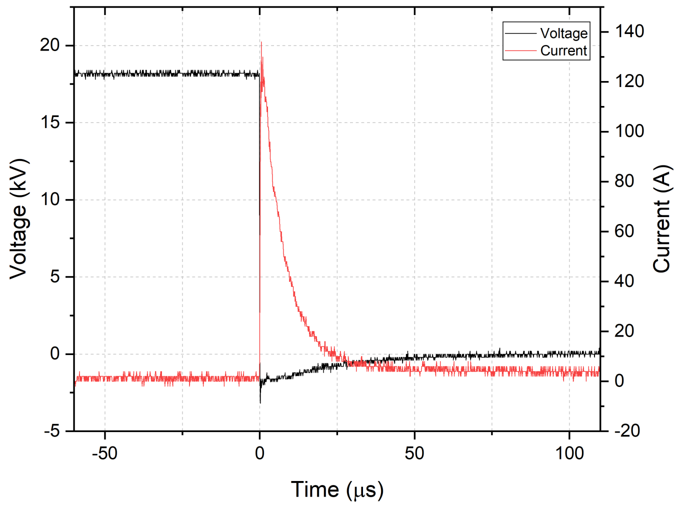

(a)

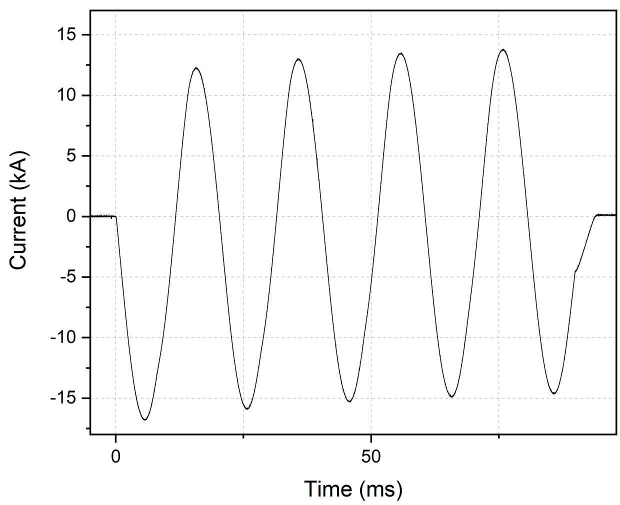

(b)

Figure 3.2: (a) High voltage test and (b) high current transformer output. For the synchronization, it is desirable to match the voltage drop with one half-cycle of current.

3.2 Test Object

The test object is a spring-type switch with axisymmetric arcing contacts. It consists of a stationary contact (pin), moving contact (tulip), main contacts, position sensor, spring and a solenoid electromagnet. The spring is compressed and held in position by the electromagnet. When the magnet is released, the tulip will move towards the pin until closed position is reached. The position sensor is connected to the spring and monitors the movement. In Figure 3.3, a schematic of the test object is shown [9]. Both in open position where the electromagnet is on, and in closed position where the moving contact has been released. For simplicity, the main contacts are excluded in this figure.

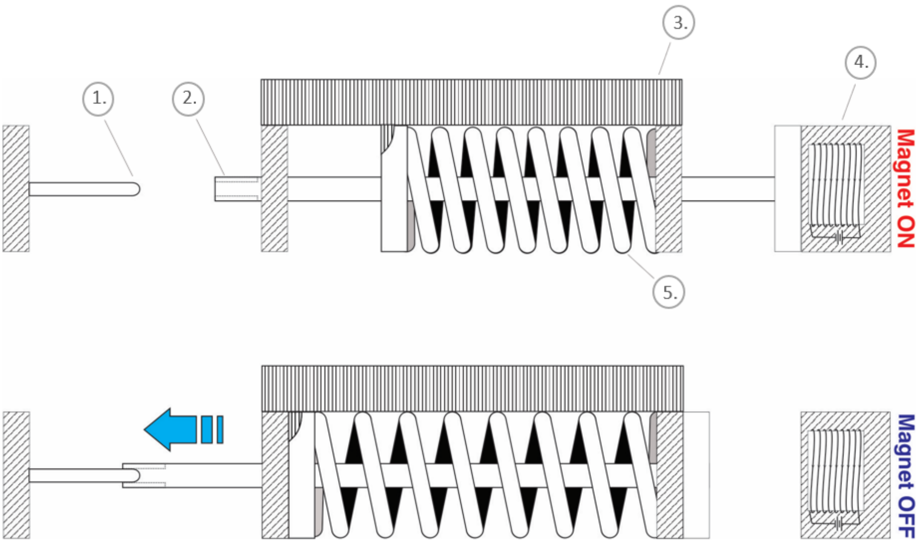

Figure 3.3: Schematic of the test object. In open (Magnet ON) and closed (Magnet OFF) position. 1. Stationary contact (cathode), 2. Moving contact (anode), 3. Position sensor, 4. Solenoid electromagnet, 5. Spring [9].

Although, the main contacts are essential for the current commutation. In Figure 3.4, a schematic of the contact setup, including both arcing and main contacts, is shown. The uppermost figure is in closed position and shows the details of the contact setup. The stationary part of the main contacts will clamp around the moving contact to secure a good connection.

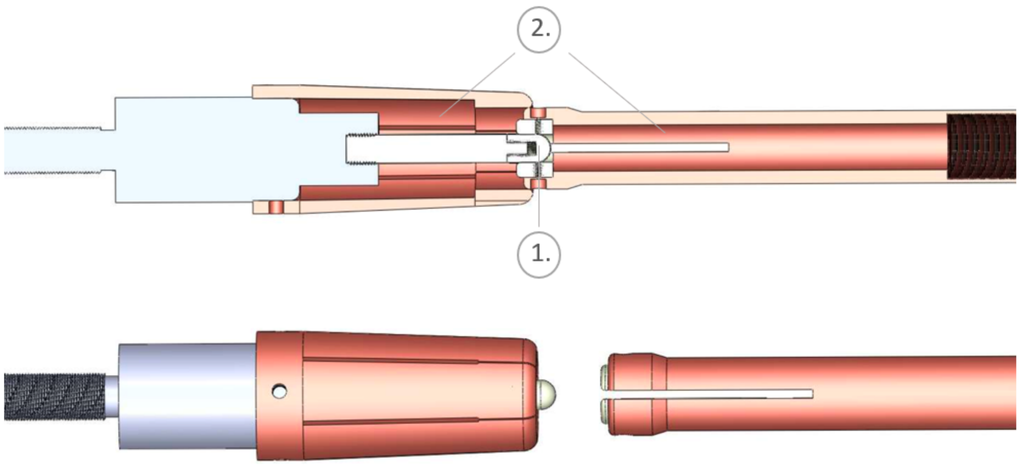

Figure 3.4: Schematic of the contact setup, both closed and open position. 1. Arcing contacts, 2. Main contacts.

The main contacts are of copper with a CuW alloy at the tip. The outer and inner diameter of the moving part is 28 mm and 20 mm, respectively. For the stationary part, the diameters are 38 mm and slightly less than 28 mm. The arcing contacts are made of a 20/80 CuW alloy.

The pin has a diameter of 10 mm and a height of 15 mm. The tulip has an outer diameter of 20 mm, and an inner diameter of slightly less than 10 mm. This is to ensure a good connection in closed position. The height of the tulip is 12.5 mm. Figure 3.5 shows a close-up of the arcing contacts.

Figure 3.5: The arcing contacts. The pin (left) and the tulip (right).

3.3 Parameters

In the experimental work, the parameters affecting the energy dissipation in the arc are important. It is essential to have control of the values to predict arc erosion behavior.

3.3.1 Pre-strike Voltage

The pre-strike voltage is supplied by the HV capacitor that is charged by the HVDC source as explained in Section 3.1.1. The HVDC source can supply a maximum of 42 kV. In this series of experiments, the pre-strike voltage is set to 20 kV for all tests. 20 kV corresponds to the peak of the phase voltage in a 24 kV system.

3.3.2 Short Circuit Current

The short circuit current is supplied from the high current transformer as described in Section 3.1.2. The transformer can supply a maximum of 60 kA. To change the current, there is an external inductance on the primary side that can be adjusted. In Figure 3.6, the equivalent circuit of a single-phase transformer is shown. The external inductance L_{ext} is also added to the circuit.

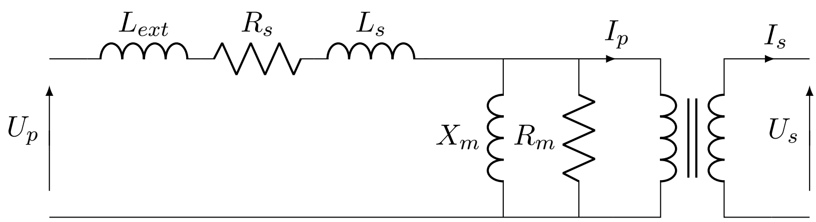

Figure 3.6: Equivalent circuit for a transformer including an external inductance.

Here, the parallel components X_m and R_m are large compared to L_{ext}, R_s and L_s and can therefore be ignored in this context. Consequently, the primary current I_p can be calculated as shown in Equation 3.1.

$$I_p = \frac{U_p}{j\omega(L_{ext} + L_s) + R_s} \tag{3.1}$$

R_s and L_s have fixed values. L_{ext} is the only part of the total impedance that is adjustable. By increasing L_{ext} it can be seen that I_p will decrease, and vice versa. The secondary current, I_s, is then a product of I_p multiplied by the turns ratio.

In this series of experiments, the inductance level is on 2 and 4. This results in currents of 22.5 kA and 14.7 kA.

3.3.3 Closing Velocity

The closing velocity is dependent on the compression of the spring in the test object. By compressing the spring in Figure 3.3 the closing velocity will increase. In this work, the compression has been 26.7 and 64.4 mm. The resulting closing velocities are 2.9 and 3.8 m/s.

3.4 Measurement Method

During the experiments, voltage, current and travel curves have been monitored. This is done by the use of an oscilloscope with an HV probe, current transformers and a position sensor. With this data, arcing time and energy dissipation can be calculated. To conclude how the different parameters affect arc erosion, other measurements are also needed.

3.4.1 Mass Loss

Mass loss is the measurement of how much of the material from the arcing contacts that have been ablated during making operation. Between each test, the contacts have been cleaned for any loose particles. Then they have been weighed after each test. The measurement has been performed with a scale with an accuracy of 0.00001 g. The mass loss measurement has been performed shortly after a test. This is to prevent oxidation that may cause measurement errors.

Chapter 4

Experimental Results and Discussion

This chapter presents the results from the experimental work. There have been four different test cases with different current levels and closing velocities. Additionally, there have been performed tests with a combination of arcing and main contacts, and only arcing contacts (without main contacts). This is to investigate the role of the main contacts in the making operation. Pre-strike arc energy and mass loss measurements have been performed for each test. The results will be discussed throughout this chapter.

4.1 Test Cases

The experiments have been divided into four different cases that have been investigated. All cases have been performed with a breakdown voltage of 20 kV, which is equivalent to the maximum rated operation voltage for medium voltage LBSs. The experiments are designed for different closing velocities and short circuit current levels. Table 4.1 presents an overview of all four cases. Regarding the current, the value is the mean recorded current amplitude. The reason for reporting the mean value is discussed in Section 4.2.

Table 4.1: Four cases for experimental testing. Different combinations of closing velocity and short circuit current. Applied breakdown voltage of 20 kV for all four cases.

Case No.	Closing Velocity [m/s]	Current Amplitude [kA]
1.	2.9	15.7
2.	2.9	21.3
3.	3.8	21.3
4.	3.8	15.7

There have been performed a series of experiments both with and without main contacts. For all cases, there have been 4-5 samples. For the experiments with arcing and main contacts, seven making operations have been conducted on each specific sample before welding was achieved. For the experimental series without main contacts, welding was achieved after four making operations.

Obtained measurements and recorded data for all making operations can be found in Appendix A and B.

4.2 Challenges and Deviations in the Measurements

In the experimental work, challenges to keep the test conditions similar for all cases have been encountered. Especially, the current has been challenging to replicate. This is a result of the synchronization system accuracy of $\pm$ 0.001 s and random behavior of arc ignition due to eroded contact surfaces. In Figure 4.1, the short circuit current for the first test of all Case 2 samples with main contacts are shown. All of the curves start at 0 ms, where the electric arc is established. The duration of one half-period varies between 7.5 - 12 ms. In this specific case, the current amplitude is changing in the range of 17 - 25 kA.

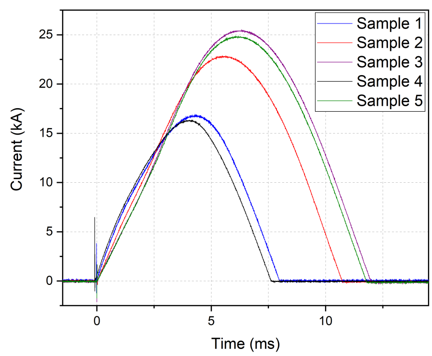

Figure 4.1: Short circuit current for the first test of all Case 2 samples with main contacts.

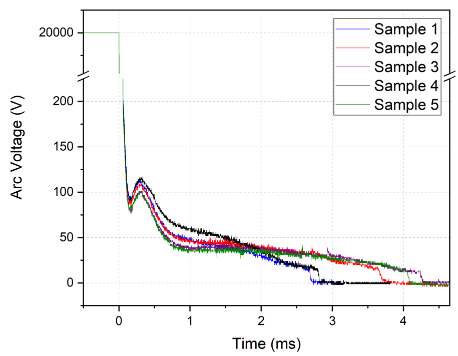

Figure 4.2: Arc voltage for the first test of all Case 2 samples with main contacts.

Figure 4.2 shows the arc voltage for the first test of all case 2 samples with main contacts. All samples start at 20 kV and rapidly decrease after the breakdown at 0 ms. An increase in arc voltage is recorded for all tests after the sharp voltage drop. At this time, for the specific case shown in Figure 4.2, the voltage increases to 97 - 116 V. Then the voltage decreases gradually to zero, which is the moment of touch for the arcing contacts. Exactly before zero voltage, a voltage drop of 14 V is recorded for all cases. This is the cathodic voltage drop for the CuW contacts. The arcing time for the first making operation for all the samples in Case 2 varies between 2.7 - 4.3 ms.

As previously mentioned, one of the challenges is random arc ignition. Making operation could gradually erode the contact surfaces and cause formations of sharp tips and irregularities on the contact surfaces. This will affect the arcing time and where the arc is established. Consequently, all the parameters will affect the arc energy dissipation, which is the main reason for contact erosion. With the variations in these parameters, the results will have an error margin.

4.3 Making Operation with Arcing and Main Contacts

In this section, the results obtained from the experiments including the main contacts will be presented.

4.3.1 Current, Voltage and Travel Curve

For each test, the current, voltage and travel curve have been recorded. To show the interrelation between different parameters and the measurement process, the making operation process and arc energy calculation are explained in detail for the first test of a Case 2 (sample 2) experiment.

The short circuit current is shown in Figure 4.3. The current amplitude is 22.8 kA and the duration of the half cycle is 10.7 ms. All the time labels (t_0, t_1, t_2 and t_3) are the same in Figures 4.3, 4.4 and 4.5. This is to show the interrelation between arc current and voltage during making operation.

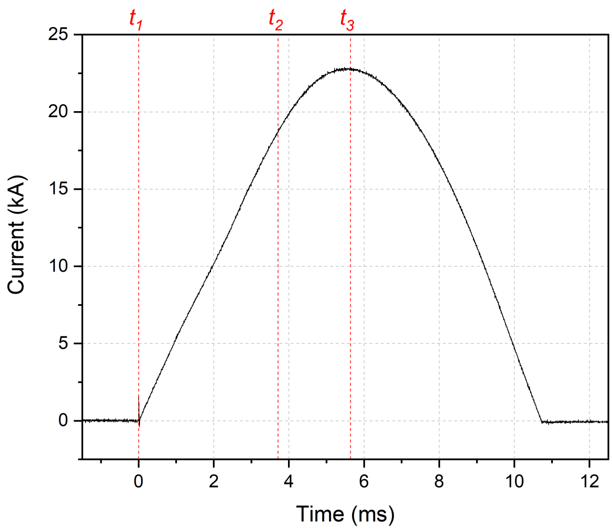

Figure 4.3: Short circuit current from a Case 2 test. At t_1, the pre-strike arc is formed. At t_2, the arcing contacts are in touch, while at t_3, the main contacts are in touch.

At t_1, the arc is established, and simultaneously the short circuit current starts to flow. Between t_1 and t_2 the current flows through the arc. At t_2, the arcing contacts are in touch. The arc is extinguished, and the current will flow through the arcing contacts. At this time, the test object continues to travel into each other until t_3, where the main contacts are in touch. Then the current commutation takes place since the main contacts are more conductive compared to the arcing contacts. Consequently, the current will mainly flow through the main contacts. The movement of the test object will continue until the stationary position is reached. The closing process is shown in the travel curve in Figure 4.5.

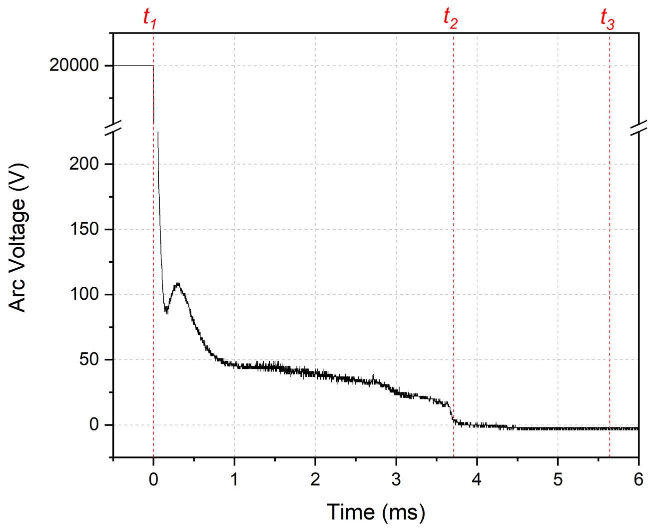

Figure 4.4: Arc voltage from a Case 2 test. At t_1, the pre-strike arc is formed. At t_2, the arcing contacts are in touch, while at t_3, the main contacts are in touch.

Figure 4.4 shows the arc voltage during the making test. The capacitor is charged up to 20 kV, which is considered as the start point of the arc voltage. After the breakdown, the voltage quickly drops to about 100 V. After approximately 1 ms, the arc has stabilized and the voltage decline is steady. The arc voltage decreases as the contacts are moving towards closed position. This is due to a short gap distance between the contacts. At t_2, the arcing contacts are in touch, and consequently, the voltage across the test object is zero.

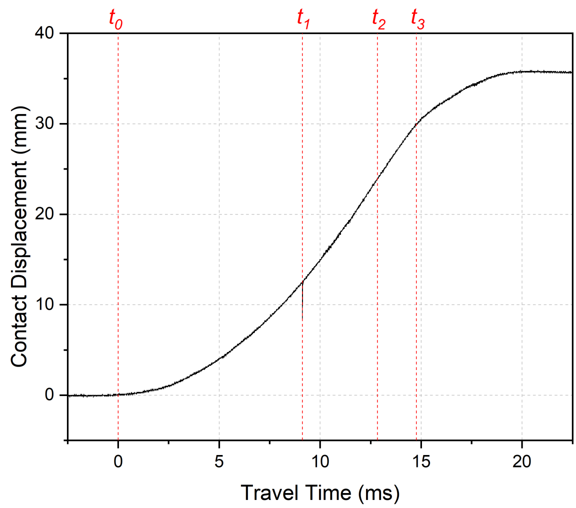

Figure 4.5: Travel curve from a Case 2 test. At t_1, the pre-strike arc is formed. At t_2, the arcing contacts are in touch, while at t_3, the main contacts are in touch. t_0 is the time of releasing the moving contact.

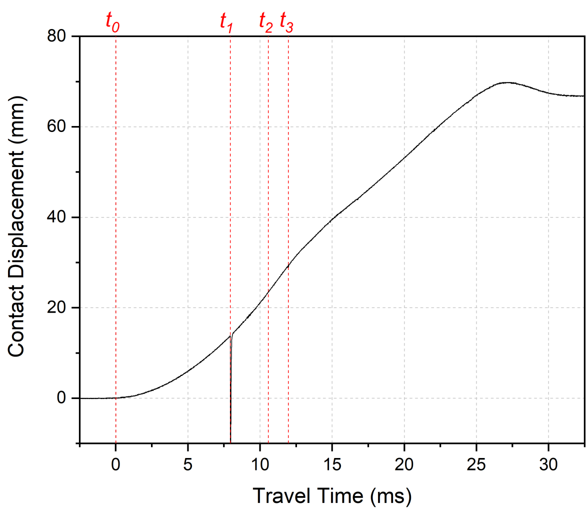

Figure 4.6: Travel curve from a Case 3 test. At t_1, the pre-strike arc is formed. At t_2, the arcing contacts are in touch, while at t_3, the main contacts are in touch. t_0 is the time of releasing the moving contact.

Figure 4.5 shows the travel curve for the Case 2 test. In this graph, t_0 is the time of releasing the moving contact by triggering the electromagnet. Accordingly, the moving contact starts to travel towards the stationary contact at this time. At t_1 the arc is established, and the current starts to flow. The arcing contacts are in touch at t_2, and the main contacts are in touch at t_3. After t_3 the steepness of the travel curve decreases, and eventually, the speed is decreased. The test object is in the fully closed position after roughly 22 ms.

To illustrate the difference of the closing process with two different closing velocities, the travel curve from a Case 3 (sample 2) test with a higher closing velocity is shown in Figure 4.6. The definition of the four time limits is the same as described in the above paragraphs. The time between t_1 and t_2, which is equal to the arcing time, is 2.6 ms, which is 1.1 ms longer than the Case 2 example. Additionally, it can be seen that the contact displacement is higher for Case 3 based on the travel curves. This is due to increased closing forces against the electromagnetic repulsion force in the arc. At higher speed, the average contact displacement is 20 mm longer than the lower speed tests.

By using Equation 2.1, the arc energy has been calculated. For Case 2 presented above, the arc energy is measured to 1152 J, with an arcing time of 3.7 ms. This resulted in a mass loss of 42.8 mg after the first test. In Table 4.2, the arcing time and arc energy for the Case 2 sample can be seen for all seven times of repeating the making operation at the same test conditions. The corresponding eroded surfaces are also shown in the table. After the second test, formations of metal droplets appeared on the contact surface. This indicates that the temperature of the metallic surface has reached above the melting point of the CuW alloy. Deformations of both pin and tulip can also be observed by repeating the test. This may cause a bad connection between the arcing contacts. After the fifth test, visible cracks have developed at the surface. After the seventh test, the arcing contacts were welded and the test object was not able to open properly.

Table 4.2: Arcing time, arc energy and eroded surface (front of pin, top of pin and top of tulip) after each test of a Case 2 sample.

Test	Measured Data	Eroded Surface
1st	Arcing time: 3,7 ms Arc energy: 1152 J	
2nd	Arcing time: 4.8 ms Arc energy: 2569 J	
3rd	Arcing time: 5.2 ms Arc energy: 2606 J	
4th	Arcing time: 6.1 ms Arc energy: 3420 J	
5th	Arcing time: 6.2 ms Arc energy: 3483 J	
6th	Arcing time: 5.5 ms Arc energy: 3007 J	
7th	Arcing time: 5,8 ms Arc Energy: 2672 J	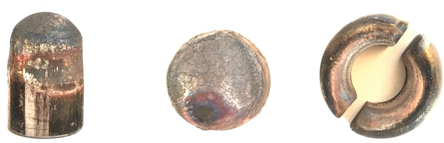

4.3.2 Mass Loss

In Figures 4.7 - 4.14, the mass loss for each case is shown. Both the average mass loss for all the cases after each test, and the mass loss as a function of arcing time.

Case 1

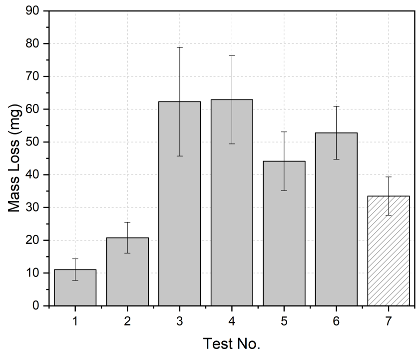

Figure 4.7: Mass loss after each number of making test for Case 1.

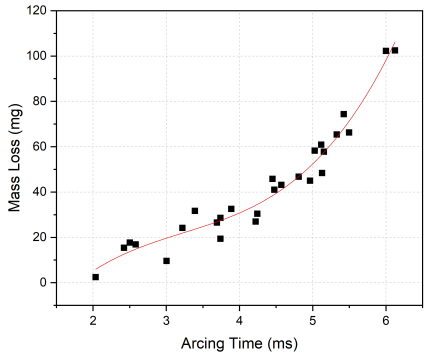

Figure 4.8: Mass loss as a function of arcing time for Case 1.

Case 2

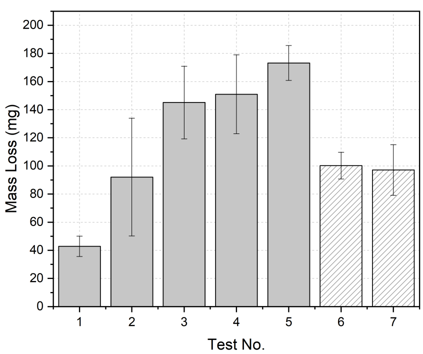

Figure 4.9: Mass loss after each number of making test for Case 2.

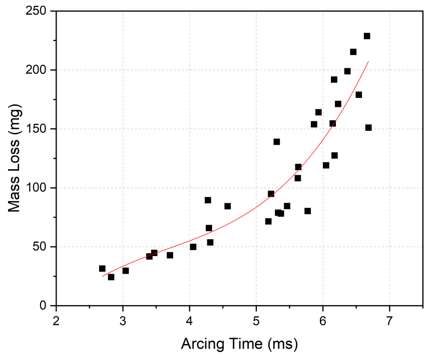

Figure 4.10: Mass loss as a function of arcing time for Case 2.

Case 3

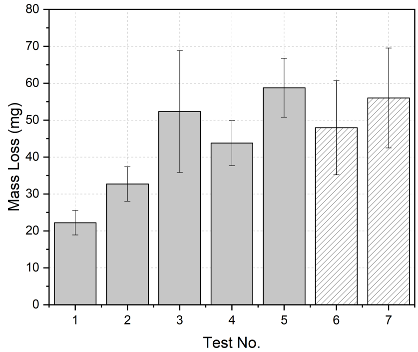

Figure 4.11: Mass loss after each number of making test for Case 3.

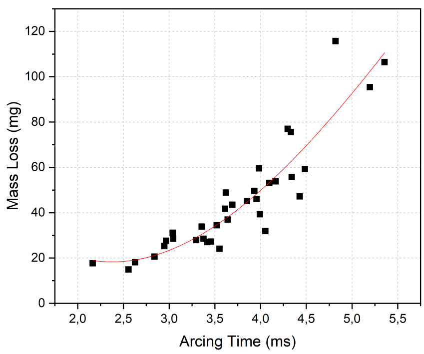

Figure 4.12: Mass loss as a function of arcing time for Case 3.

Case 4

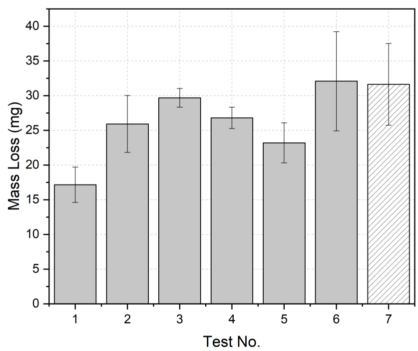

Figure 4.13: Mass loss after each number of making test for Case 4.

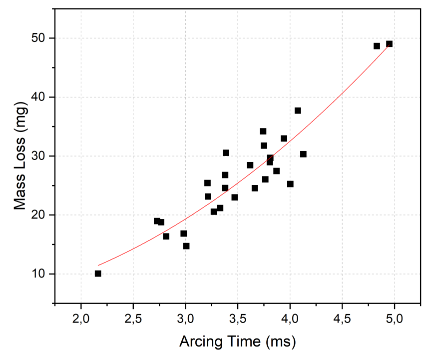

Figure 4.14: Mass loss as a function of arcing time for Case 4.

In the bar graphs, the hatched bars show the experiments where some erosion has appeared on the main contacts in addition to the arcing contacts. It could be due to deformation in the arcing contacts, and therefore a bad connection between them when the main contacts are closing. As a result, the arc is partially formed between the main contacts. Consequently, the calculated arc energy contributes to erosion on the main contacts in addition to the arcing contacts. Therefore, the total mass loss is higher than the measured number for the hatched tests.

For most of the tests, the mass loss increases after each making operation. In Case 3, the mass loss after the fourth test is smaller than the third test. It could be a result of arc ignition from a new area that has little degradation before the earlier test. In this case, the arc energy and time are smaller compared to the earlier tests.

For all cases, a clear tendency is that the mass loss has an exponential increase related to arcing time. The increase is expected, as a longer arcing time results in a prolonged exposure time to high temperatures for the contact surfaces. At very high temperatures, the contact surface will start to melt and vaporize.

Total Mass Loss

In Figure 4.15, the total mass loss for each case is shown. Case 4, with the highest speed and lowest current, has the lowest amount of mass loss. For Cases 1 and 3, the mass loss is close to similar. Case 1 is exposed to a lower current with a lower closing velocity compared to Case 3. As expected, the worst-case scenario has the highest mass loss. Case 2 has the lowest speed and highest current, resulting in the highest arc energy dissipation between the arcing contacts. For this case, the mass loss is approximately 2.5 times higher than Cases 1 and 3.

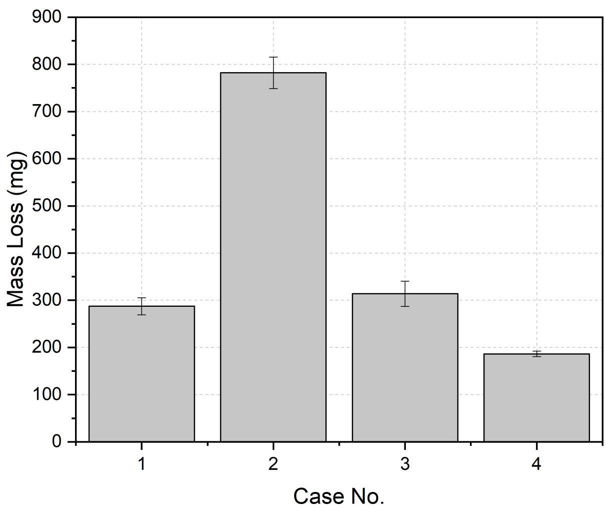

Figure 4.15: The total mass loss for each case after 7 tests.

4.3.3 Welding During Making Operation

Predictably, the arc energy is dependent on the arcing time. The relation between arc energy and arcing time is shown in Figure 4.16. Referring to Equation 2.1, arc voltage (Figure 4.4) and short circuit current (Figure 4.3), an increase in arcing time results in a current increase in the order of kiloamperes, and arc voltage decrease to the order of a few volts. Therefore, the arc energy increases by arcing time, which is experimentally shown below.

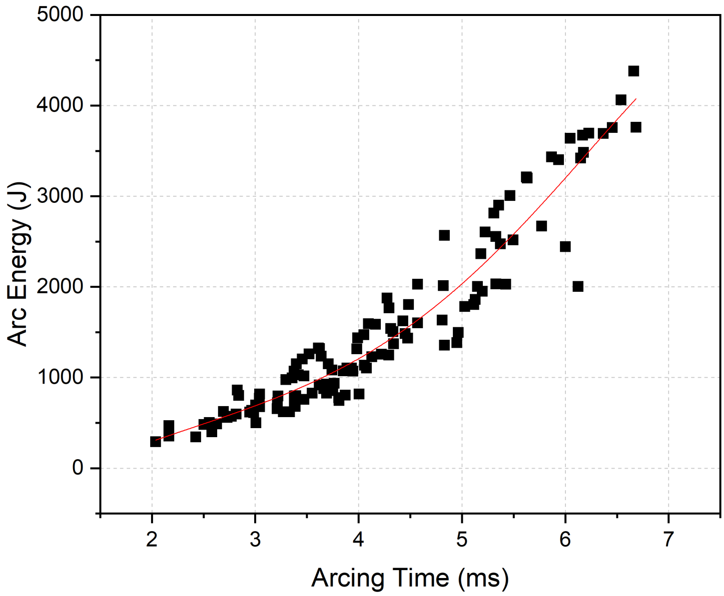

Figure 4.16: Arc Energy as a function of Arcing Time for all tests with main contacts.

Figures 4.17 and 4.18 show the mass loss related to arc energy for the different closing velocities.

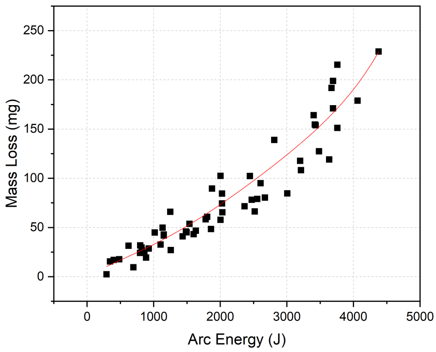

Figure 4.17: Mass Loss as a function of Arc Energy at closing velocity of 2.9 m/s.

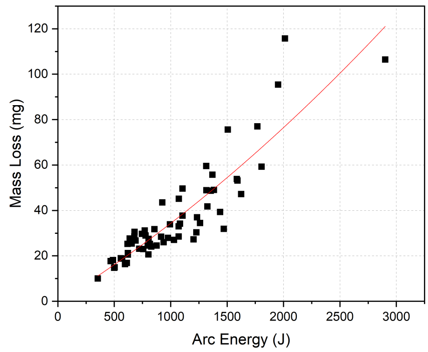

Figure 4.18: Mass Loss as a function of Arc Energy at closing velocity of 3.8 m/s.

An increase in arc energy causes a higher mass loss which can be seen for both closing velocities. By increasing the closing speed, there is less arc energy, and consequently, less mass loss compared to the lower closing velocity.

In the experimental series with the main contacts, welding was only achieved under Case 2 conditions. At these conditions, welding was reached at two out of five samples after seven repeated tests. In Table B.2 in Appendix B, it can be seen that the arc energy for the seventh test is not necessarily the highest for each sample series. This shows that arc energy is not the only factor for welding. Consequently, welding depends on arc energy and also the degree of contact erosion from previous making operations. For a higher closing velocity, a higher number of tests is required to reach sufficient arc energy and erosion that will result in welding.

4.4 Making Operation with Arcing Contacts

In this section, the results obtained from the experiments with only the arcing contacts will be presented.

4.4.1 Current, Voltage and Travel Curve

The short circuit current of the fourth sample of Case 2 is shown in Figure 4.19. The current amplitude is 21.5 kA with a half-cycle duration of 10.56 ms. As explained in Section 4.2, some deviations in the parameters like short circuit current and arc voltage will occur. In the following graphs, there is no t_3 since the main contacts are removed from the test object. The other time labels, however, represent the same. t_1 and t_2 are the time of breakdown and arcing contacts in touch, respectively. For the travel curve, t_0 is the time of releasing the moving contact by triggering the electromagnet.

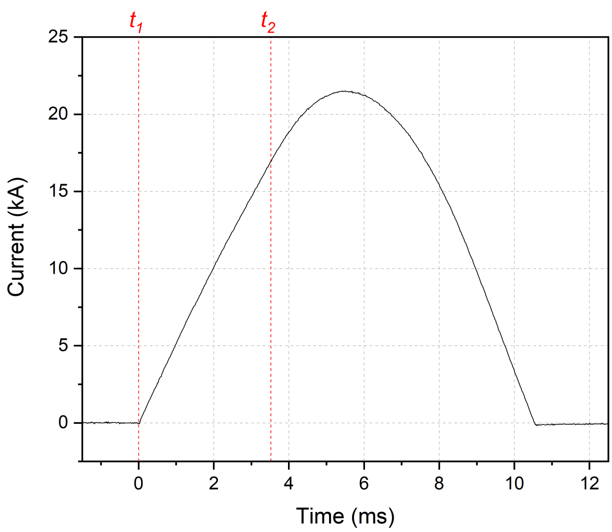

Figure 4.19: Short circuit current from a Case 2 test. At t_1, the pre-strike arc is formed. At t_2, the arcing contacts are in touch.

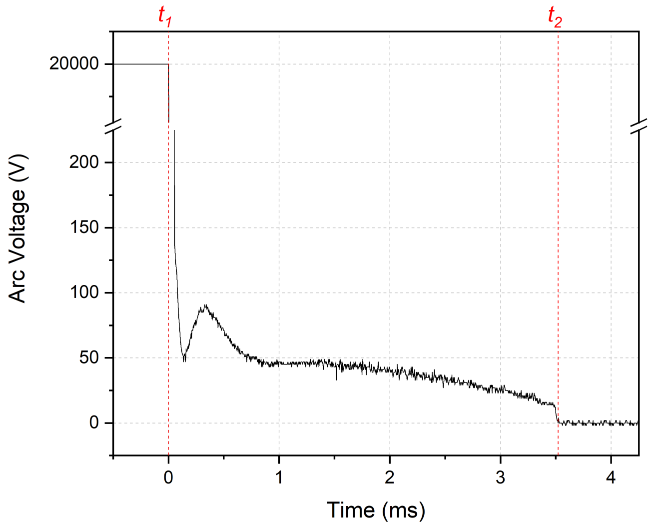

Figure 4.20: Arc voltage from a Case 2 test. At t_1, the pre-strike arc is formed. At t_2, the arcing contacts are in touch.

Figure 4.20 shows the arc voltage. It resembles the arc voltage in Section 4.3.1. There is a sharp drop when the breakdown occurs. During the first millisecond, the arc is unstable and the voltage increases from 50 to 80 V. Then, the voltage decreases steadily as the moving contact approaches the stationary one. After the arcing contacts are in touch, the arc voltage is 0 V.

In Figure 4.21, the related travel curve is shown. The contact displacement of 35 mm is similar to the experiment with main contacts. The timing is also similar. In this curve, however, the travel curve overshoots before stabilizing in the closed position. In this case, there are no main contacts to clamp and slow down the contact movement. Therefore, the contact continues to travel before bouncing back in the closed position.

Figure 4.22 shows a sample with higher speed and without the main contacts. There are no significant differences compared to Figure 4.6. This travel curve is recorded for the first test for the second sample of Case 3.

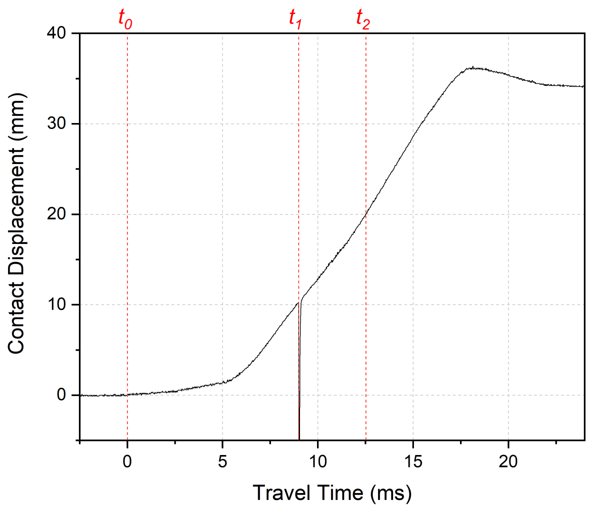

Figure 4.21: Travel curve from a Case 2 test. The moving contact is released at t_0. At t_1, the pre-strike arc is formed. At t_2, the arcing contacts are in touch.

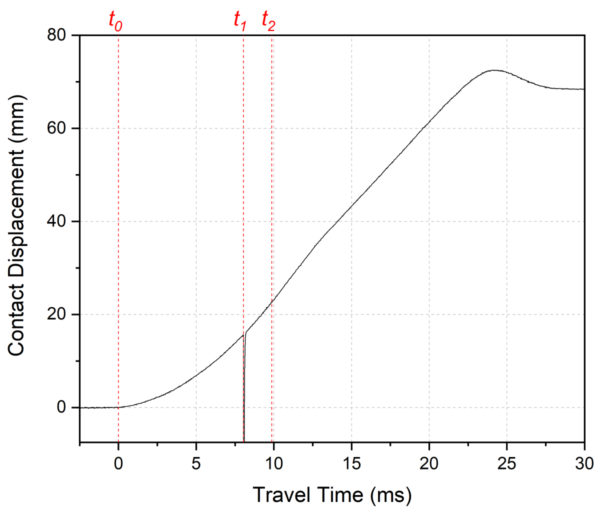

Figure 4.22: Travel curve from a Case 3 test. The moving contact is released at t_0. At t_1, the pre-strike arc is formed. At t_2, the arcing contacts are in touch.

In Table 4.3, the arcing time and arc energy are put in order for the Case 2 samples for all four times of repeating the making operation. Additionally, pictures of the eroded surfaces are included. The tendency is similar to the samples with main contacts. There are formations of droplets on the surface after the first test. After the third test, there are visible cracks on the pin. Welding was achieved after the fourth making test without the main contacts.

Table 4.3: Arcing time, arc energy and eroded surface (front of pin, top of pin and top of tulip) after each test of a Case 2 sample (without main contacts).

Test	Measured Data	Eroded Surface		
1st	Arcing time: 3,5 ms Arc energy: 1042 J			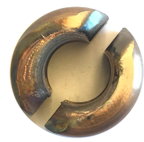
2nd	Arcing time: 5.1 ms Arc energy: 2575 J			
3rd	Arcing time: 5.4 ms Arc energy: 2935 J		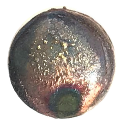	
4th	Arcing time: 5.5 ms Arc energy: 2746 J			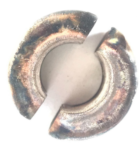

4.4.2 Mass Loss

In Figures 4.23 - 4.30, the result of the mass loss measurement is shown. The bar charts show the average mass loss after each test for the four cases. Additionally, the mass loss as a function of arcing time is plotted.

Case 1

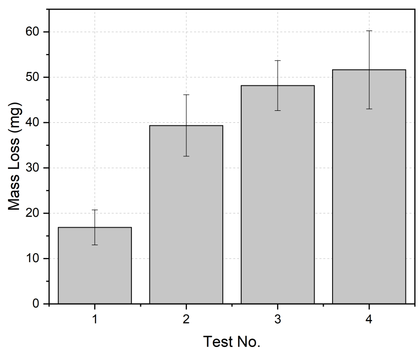

Figure 4.23: Mass loss after each number of making test for Case 1.

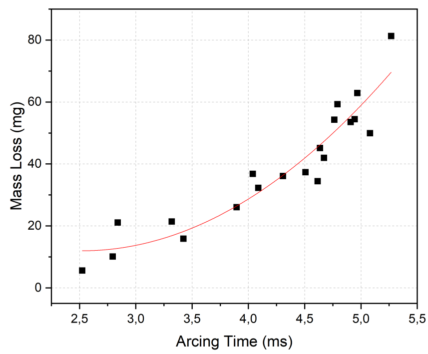

Figure 4.24: Mass loss as a function of arcing time for Case 1.

Case 2

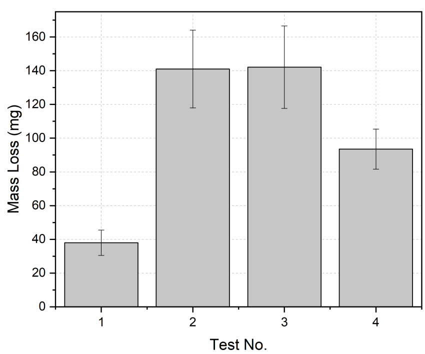

Figure 4.25: Mass loss after each number of making test for Case 2.

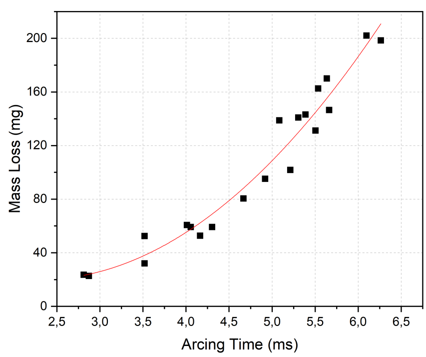

Figure 4.26: Mass loss as a function of arcing time for Case 2.

Case 3

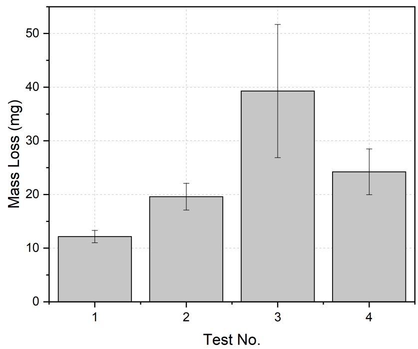

Figure 4.27: Mass loss after each number of making test for Case 3.

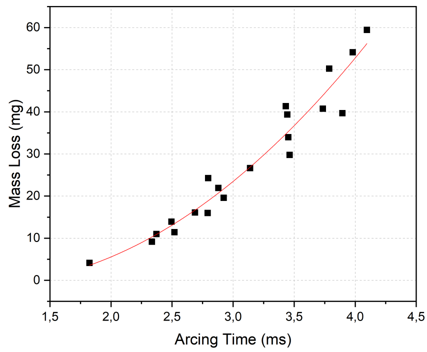

Figure 4.28: Mass loss as a function of arcing time for Case 3.

Case 4

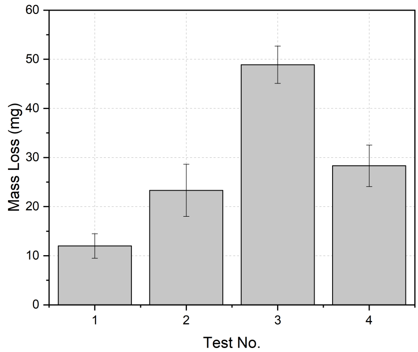

Figure 4.29: Mass loss after each number of making test for Case 4.

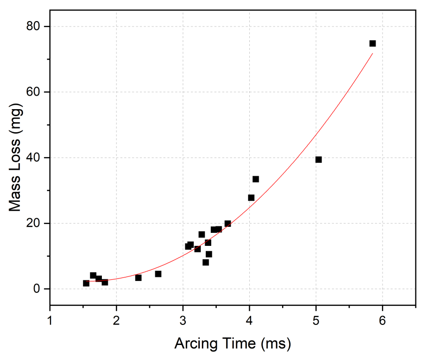

Figure 4.30: Mass loss as a function of arcing time for Case 4.

For all cases, the mass loss increases by each test for the first three rounds of experiments. For the fourth test, however, the mass loss decreases in Cases 2, 3 and 4. Referring to Appendix B, lower mass loss observed for Cases 2, 3 and 4 for the fourth time of repeating the making test corresponds to lower arcing energy compared to the previous test. It could be due to burned contact surfaces after three times of tests and the absence of any sharp points. It could also be a consequence of the uncertainty in the test conditions as explained in Section 4.2. Apart from that, the mass loss tendency during making operation is quite similar to the tests with the main contacts.

Total Mass Loss

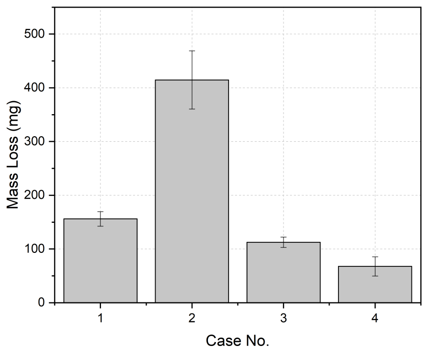

Figure 4.31: Total mass for loss each case after four tests without main contacts.

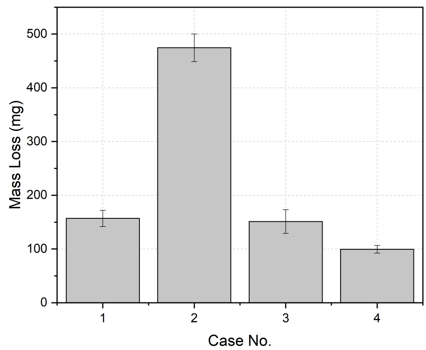

Figure 4.32: Total mass loss for each case after the fourth test with main contacts.

Figures 4.31 and 4.32 show the total mass loss after four tests with and without main contacts, respectively. By comparing these two plots, it can be seen that the mass loss is close to similar. This indicates that the mass loss is minimally affected by the main contacts. Therefore, the mass loss of arcing contacts is mainly caused by arc burning. The presence of the main contacts will prevent contact welding after four times of making operations. This is because parts of the short circuit current will flow through the main contacts when the switch is in the closed position. However, the main contacts are not the permanent solution to avoid switch failure. With the presence of main contacts, the arcing contacts were welded after seven times of repeating the making test.

4.4.3 Welding During Making Operation

In Figure 4.33, the relation between arc energy and arcing time is shown for making operation with only the arcing contacts. The data points are collected for every single test for all four cases. The fitted red graph is almost identical to the one in Figure 4.16.

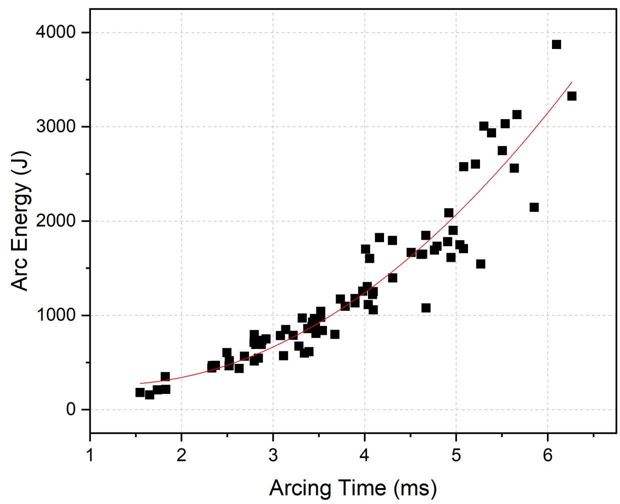

Figure 4.33: Arc Energy as a function of Arcing Time for all tests without main contacts.

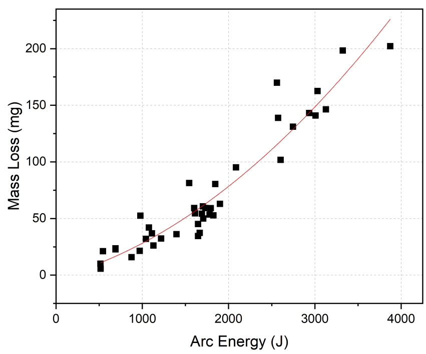

Figure 4.34: Mass Loss as a function of Arc Energy at closing velocity of 2.9 m/s.

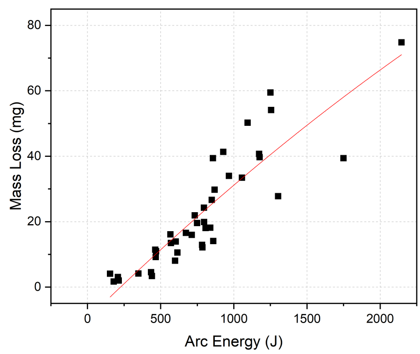

Figure 4.35: Mass Loss as a function of Arc Energy at closing velocity of 3.8 m/s.

In Figures 4.34 and 4.35, the mass loss is plotted as a function of arc energy for each closing velocity without main contacts. No welding was achieved at the samples with the closing speed of 3.8 m/s. For Case 2, with the lower closing speed and higher short circuit current, three out of five samples were welded after four tests. Compared to Figure 4.17 and 4.15, the number of repeating the making test to reach welding has decreased without main contacts. Consequently, main contacts will extend the lifetime of the switch.

Chapter 5

Conclusion

In the experimental work performed in this thesis, there have been performed making operations with short circuit currents at LBSs. The degradation effects on the arcing contacts have been investigated. Tests have been performed with and without main contacts, and four different combinations of test conditions, in total eight different tests, repeated 4-7 times with 4-5 samples. After analyzing and discussing the obtained results, the following conclusions can be drawn:

- If an LBS, including both arcing and main contacts, is exposed to short circuit currents of 20 kA with a closing velocity of 2.9 m/s, there is a probability that the arcing contacts will be welded after six or seven making operations. As a result, the switch will not operate properly during the next interrupting operation.
- Higher short circuit currents will increase the erosion on the arcing contacts. At a closing velocity of 2.9 m/s, the total mass loss was approximately three times higher at a short circuit current of 21.3 kA compared to 15.7 kA.
- By increasing the closing velocity from 2.9 m/s to 3.8 m/s during making operation, the arc energy will decrease. Consequently, the mass loss and erosion will decrease, and the lifetime of the switchgear will be extended. During making tests at higher velocities, no samples were welded.

- The main contacts play an essential role during making operation and can increase the lifetime of the switch. However, there is still a probability of switch failure with main contacts after several making operations. With the main contacts, the arcing contacts were welded after seven making operations. Without the main contacts, welding was achieved after four making operations.

- The welding of arcing contacts is dependent on both arc energy and the degree of contact erosion that gradually occurs by repeated making operation.

Chapter 6

Further Work

Based on the discussion and conclusion, suggestions for further work are:

- The obtained results from this thesis show that a higher closing velocity is preferable during making operation. However, it is uncertain if the closing speed will affect the current interruption. Therefore, it is a point of interest to investigate how a higher closing velocity would impact the current interruption process.
- Utilize other, environmentally friendly gases as interrupting medium and investigate the performance during making operation. It would be of great interest to conduct similar experimental work with AirPlus as the interrupting medium.
- Perform making tests with different geometries for the arcing contacts. It could be interesting to try different shapes of arcing contacts to see how this will affect erosion. Additionally, the material of the arcing contacts could be changed.
- Look into different designs and try other materials for the main contacts. After observing erosion on the main contacts, it would
- Carry out experiments with more focus on the main contacts. It would be interesting to look at different designs and materials of the main contacts to reduce erosion during current making.

Bibliography

[1] Metals Comparenature, "Compare properties." `https://metals.comparenature.com/`. (Online; accessed 15 April 2021).

[2] J. J. Shea, "High current ac break arc contact erosion," in *2008 Proceedings of the 54th IEEE Holm Conference on Electrical Contacts*, pp. xxii–xlvi, 2008.

[3] K. Niayesh and M. Runde, *Power Switching Components*. Springer, 2017.

[4] A. A. Razi-Kazemi, K. Niayesh, and R. Nilchi, "A probabilistic model-aided failure prediction approach for spring-type operating mechanism of high-voltage circuit breakers," *IEEE Transactions on Power Delivery*, vol. 34, no. 4, pp. 1280–1290, 2019.

[5] J. Tepper, M. Seeger, T. Votteler, V. Behrens, and T. Honig, "Investigation on erosion of cu/w contacts in high-voltage circuit breakers," *IEEE Transactions on Components and Packaging Technologies*, vol. 29, no. 3, pp. 658–665, 2006.

[6] Z. Wang, *Study on the Mechanisms and Prediction Methods of Arcing Contact Erosion of High-voltage SF6 Circuit Breaker*. PhD thesis, University of Liverpool, 2018.

[7] IEC, "High-voltage switchgear and controlgear - part 101: Synthetic testing," International Electrotechnical Commission, Geneva, Switzerland, IEC 62271-101:2012, 2012.

[8] N. Dorraki and K. Niayesh, "Optical investigation on pre-strike arc characteristics in medium-voltage load break switches," *J. Phys. D: Appl. Phys.*, vol. 54, 04 2021.

[9] N. Dorraki and K. Niayesh, “Spectroscopic investigation of metal content in prestrike arc during making operation in a low-current model switch,” *IEEE Transactions on Plasma Science*, vol. 48, no. 10, pp. 3698–3704, 2020.

[10] M. Strand, “Contact Degradation in Air Load Break Switches by Making Operation Under Short Circuit Condition,” project report in TET4510, Department of Electric Power Engineering, NTNU – Norwegian University of Science and Technology, Dec. 2020.

[11] E. Ilstad, *Insulating Materials for High Voltage Applications, Digital Compendium*. NTNU, Department of Electric Power Engineering, 08 2018.

[12] H. M. Ryan, *High voltage engineering and testing*. London: Institution of Electrical Engineers, 2nd ed., 2001.

[13] A. Janssen, D. Makareinis, and C. Sölver, “International surveys on circuit-breaker reliability data for substation and system studies,” *IEEE Transactions on Power Delivery*, vol. 29, no. 2, pp. 808–814, 2014.

[14] P. G. Slade, *Electrical Contacts*. CRC Press, 2nd ed., 2014.

[15] S. Kharin, H. Nouri, and D. Amft, “Dynamics of arc phenomena at closure of electrical contacts in vacuum circuit breakers,” *Plasma Science, IEEE Transactions on*, vol. 33, pp. 1576 – 1581, 11 2005.

[16] K. Hotta and T. Inaguchi, “Dependence of contact weld force on arc energy supplied to contact surface in low voltage switches,” in *2015 IEEE 61st Holm Conference on Electrical Contacts (Holm)*, pp. 160–165, 2015.

[17] T. Mutzel, M. Bender, and R. Niederreuther, “The effect of material composition on dynamic welding of electrical contacts,” in *2013 IEEE 59th Holm Conference on Electrical Contacts (Holm 2013)*, pp. 1–7, 2013.

[18] W. R. Wilson, “High-current arc erosion of electric contact materials [includes discussion],” *Transactions of the American Institute of Electrical Engineers. Part III: Power Apparatus and Systems*, vol. 74, no. 3, pp. 657–664, 1955.

[19] N. Dorraki, M. Strand, and K. Niayesh, “Impact of pre-strike arc on contacts degradation after short circuit current making operation in medium voltage air load break switches,” *ICEC - International Conference on Electrical Contacts*, 12 2020.

[20] L. G. Christophorou, J. K. Olthoff, and D. S. Green, “Gases for electrical insulation and arc interruption: Possible present and future alternatives to pure SF_6,” *NIST Standard Reference Simulation Website*, pp. 6–10, 1997.

[21] G. Myhre, D. Shindell, F.-M. Bréon, W. Collins, J. Fuglestvedt, J. Huang, D. Koch, J.-F. Lamarque, D. Lee, B. Mendoza, T. Nakajima, A. Robock, G. Stephens, T. Takemura, and H. Zhang, “Climate change 2013: The physical science basis. contribution of working group I to the fifth assessment report of the intergovernmental panel on climate change [Stocker, T.F., D. Qin, G.-K. Plattner, M. Tignor, S.K. Allen, J. Boschung, A. Nauels, Y. Xia, V. Bex and P.M. Midgley (eds.)],” *Anthropogenic and Natural Radiative Forcing.*, 2013.

[22] N. S. Aanensen, E. Jonsson, and M. Runde, “Air-flow investigation for a medium-voltage load break switch,” *IEEE Transactions on Power Delivery*, vol. 30, no. 1, pp. 299–306, 2015.

[23] P. C. Stoller, M. Seeger, A. A. Iordanidis, and G. V. Naidis, “CO_2 as an arc interruption medium in gas circuit breakers,” *IEEE Transactions on Plasma Science*, vol. 41, no. 8, pp. 2359–2369, 2013.

[24] S. Kosse, P. Nikolic, and G. Kachelriess, “Holistic evaluation of the performance of today’s sf6 alternatives proposals,” *CIRED - Open Access Proceedings Journal*, vol. 2017, pp. 210–213, 10 2017.

[25] ABB, “AirPlus TM: An alternative to SF6 as an insulation and switching medium in electrical switchgear.” `https://library.e.abb.com/public/3405a31190934a8c98997eca8fc811be/ABB%20Review%202-2016_AirPlus_An%20Alternative%20to%20SF6.pdf`. Online; accessed 29 April 2021.

Appendix A

Mass Loss

Table A.1: Mass Loss [mg] for Case 1 (With main contacts)

Sample		Control	1st	2nd	3rd	4th	5th	6th	7th	Total Mass Loss
1	**Pin**	13802.42	13804.82	13798.97	13790.12	13750.51	13740.03	13730.48	13711.81	90.61
	Tulip	38611.99	38600.23	38588.42	38570.73	38508.13	38488.16	38450.94	38428.62	183.37
	Pin + Tulip	52414.41	52405.05	52387.39	52360.85	52258.64	52228.19	52181.42	52140.43	273.98
	Difference		9.36	17.66	26.54	102.21	30.45	46.77	40.99	
2	**Pin**	13744.49	13742.4	13730.55	13693.63	13674.83	13667.66	13641.64	13625.15	119.34
	Tulip	38592.51	38577.69	38557.85	38492.33	38462.76	38442.98	38403.62	38375.14	217.37
	Pin + Tulip	52337	52320.09	52288.4	52185.96	52137.59	52110.64	52045.26	52000.29	336.71
	Difference		16.91	31.69	102.44	48.37	26.95	65.38	44.97	
3	**Pin**	13535.51	13535.31	13532.4	13505.74	13491.57	13469.83	13454.42	13443.49	92.02
	Tulip	38634.09	38631.86	38625.19	38577.47	38548.51	38509.39	38492.22	38474.59	159.5
	Pin + Tulip	52169.6	52167.17	52157.59	52083.21	52040.08	51979.22	51946.64	51918.08	251.52
	Difference		2.43	9.58	74.38	43.13	60.86	32.58	28.56	
4	**Pin**	13806.49	13804.78	13800.4	13788.95	13768	13744.32	13719.98	13712.47	94.02
	Tulip	38597.33	38583.64	38563.83	38529.47	38492.6	38458.04	38416.09	38404.23	193.1
	Pin + Tulip	52403.82	52388.42	52364.23	52318.42	52260.6	52202.36	52136.07	52116.7	287.12
	Difference		15.4	24.19	45.81	57.82	58.24	66.29	19.37	

Table A.2: Mass Loss [mg] for Case 2 (With main contacts)

Sample		Control	1st	2nd	3rd	4th	5th	6th	7th	Total Mass Loss
1	**Pin**	13737.04	13725.57	13710.78	13633.61	13569.24	13489.59	13458.2	13389.14	347.9
	Tulip	38580.73	38560.71	38533.77	38419.12	38329.59	38219.47	38179.31	38097.29	483.4
	Pin + Tulip	52317.77	52286.28	52244.55	52052.73	51898.83	51709.06	51637.51	51486.43	831.34
	Difference		31.49	41.73	191.82	153.9	189.77	71.55	151.08	
2	**Pin**	13717.4	13706.44	13593.24	13552.15	13487.27	13431.04	13393.81	13355.51	361.89
	Tulip	38816.53	38784.68	38643.21	38589.39	38499.66	38428.44	38381.15	38339.13	477.4
	Pin + Tulip	52533.93	52491.12	52236.45	52141.54	51986.93	51859.48	51774.96	51694.64	839.29
	Difference		42.81	254.67	94.91	154.61	127.45	84.52	80.32	
3	**Pin**	13723.66	13695.44	13661.31	13569.55	13548.22	13466.61	13412.28		311.38
	Tulip	38773.68	38736	38680.59	38557.03	38524.73	38435.24	38381.4	*Welded at*	392.28
	Pin + Tulip	52497.34	52431.44	52341.9	52126.58	52072.95	51901.85	51793.68	*6th test*	703.66
	Difference		65.9	89.54	215.32	53.63	171.1	108.17		
4	**Pin**	13718.37	13712.34	13702.34	13672.88	13607.24	13519.55	13459.83	13424.33	294.04
	Tulip	38470.47	38452.32	38432.68	38377.7	38279.29	38168.14	38110.21	38066.81	403.66
	Pin + Tulip	52188.84	52164.66	52135.02	52050.58	51886.53	51687.69	51570.04	51491.14	697.7
	Difference		24.18	29.64	84.44	164.05	198.84	117.65	78.9	
5	**Pin**	13527.76	13518.69	13498.36	13442.24	13355.59	13273.99	13216.91	13181.56	346.2
	Tulip	38810.37	38769.64	38745.19	338662.33	38520.29	38423.03	38361	38318.23	492.14
	Pin + Tulip	52338.13	52288.33	52243.55	52104.57	51875.88	51697.02	51577.91	51499.79	838.34
	Difference		49.8	44.78	138.98	228.69	178.86	119.11	78.12	

Table A.3: Mass Loss [mg] for Case 3 (With main contacts)

Sample		Control	1st	2nd	3rd	4th	5th	6th	7th	Total Mass Loss
1	**Pin**	13592.59	13588.96	13575.55	13564.89	13550.23	13536.02	13518.17	13495.14	97.45
	Tulip	38612.17	38598.13	38562.69	38545.7	38518.58	38495.84	38467.69	38436.87	175.3
	Pin + Tulip	52204.76	52187.09	52138.24	52110.59	52068.81	52031.86	51985.86	51932.01	272.75
	Difference		17.67	48.85	27.65	41.78	36.95	46	53.85	
2	**Pin**	13676.07	13673.55	13667.12	13651.53	13642.93	13611.77	13599.32	13579.43	96.64
	Tulip	38729.18	38713.58	38699.42	38671.49	38646.23	38600.42	38585.84	38552.58	176.6
	Pin + Tulip	52405.25	52387.13	52366.54	52323.02	52289.16	52212.19	52185.16	52132.01	273.24
	Difference		18.12	20.59	43.52	33.86	76.97	27.03	53.15	
3	**Pin**	13652.6	13643.75	13635.25	13583.32	13559.36	13541.24	13525.07	13511.22	141.38
	Tulip	38778.04	38755.03	38729.08	38665.3	38633.5	38592.36	38561.31	38535.86	242.18
	Pin + Tulip	52430.64	52398.78	52364.33	52248.62	52192.86	52133.6	52086.38	52047.08	383.56
	Difference		31.86	34.45	115.71	55.76	59.26	47.22	39.3	
4	**Pin**	13608.8	13601.15	13590.97	13572.13	13564.52	13537.27	13526.59	13517.91	90.89
	Tulip	38644.61	38623.76	38602.78	38572	38551.68	38503.64	38489.94	38471.35	173.26
	Pin + Tulip	52253.41	52224.91	52193.75	52144.13	52116.2	52040.61	52016.53	51989.26	264.15
	Difference		28.5	31.16	49.62	27.93	75.59	24.08	27.27	
5	**Pin**	13619.66	13617.83	13612.28	13603.88	13581.44	13566.4	13526.01	13480.75	138.91
	Tulip	38564	38550.87	38527.94	38511.11	38473.99	38443.87	38388.88	38327.71	236.29
	Pin + Tulip	52183.66	52168.7	52140.22	52114.99	52055.43	52010.27	51914.89	51808.46	375.2
	Difference		14.96	28.48	25.23	59.56	45.16	95.38	106.43	

Table A.4: Mass Loss [mg] for Case 4 (With main contacts)

Sample		Control	1st	2nd	3rd	4th	5th	6th	7th	Total Mass Loss
1	**Pin**	13548.41	13545.62	13539.61	13527.16	13516.62	13506.72	13504.11	13491.23	57.18
	Tulip	38581.54	38567.49	38541.75	38523.65	38505.25	38487.71	38473.97	38456.54	125
	Pin + Tulip	52129.95	52113.11	52081.36	52050.81	52021.87	51994.43	51978.08	51947.77	182.18
	Difference		16.84	31.75	30.55	28.94	27.44	16.35	30.31	
2	**Pin**	13627.27	13622.06	13613.44	13604.24	13593.49	13588.17	13578.65	13572.2	55.07
	Tulip	38582.24	38566.27	38540.69	38521.46	38502.53	38493.14	38477.42	38460.9	121.338
	Pin + Tulip	52209.51	52188.33	52154.13	52125.7	52096.02	52081.31	52056.07	52033.1	176.408
	Difference		21.18	34.2	38.43	29.68	14.71	25.24	22.97	
3	**Pin**	38574.46	38558.79	38546.232	38521.37	38506.71	38485.82	38463.36	38447.16	127.3
	Tulip	13537.67	13532.8	13526.31	13518.28	13509.81	13504.67	13489.43	13481.08	56.59
	Pin + Tulip	52112.13	52091.59	52072.63	52039.65	52016.52	51990.49	51952.79	51928.24	183.89
	Difference		20.54	18.96	32.98	23.13	26.03	37.7	24.55	
4	**Pin**	13569.83	13567.96	13563.69	13555.88	13545.24	13537.62	13519.05	13497.79	72.04
	Tulip	38710.62	38702.44	38687.95	38669	38654.23	38637.29	38606.85	38579.46	131.16
	Pin + Tulip	52280.45	52270.4	52251.64	52224.88	52199.47	52174.91	52125.9	52077.25	203.2
	Difference		10.05	18.76	26.76	25.41	24.56	49.01	48.65	

Table A.5: Mass Loss [mg] for Case 1 (Without main contacts)

Sample		Control	1st	2nd	3rd	4th	Total Mass Loss
1	**Pin**	15264.68	15262.36	15250.67	15223.67	15217.60	47.08
	Tulip	37314.38	37290.64	37260.37	37218.09	37179.87	134.51
	Pin + Tulip	52579.06	52553	5211.04	52451.76	52397.47	181.59
	Difference		26.06	41.96	59.28	54.29	
2	**Pin**	15232.13	15231.52	15233.42	15221.33	15193.58	38.55
	Tulip	37300.89	37295.88	37278.11	37245.05	37191.54	109.32
	Pin + Tulip	52532.99	52527.4	52511.53	52466.38	52385.12	147.87
	Difference		5.59	15.87	45.15	81.26	-
3	**Pin**	15389.45	15387.86	15369.57	15350.77	15335.18	54.27
	Tulip	37352.28	37332.43	37296.26	37252.17	37214.24	138.04
	Pin + Tulip	52741.73	52720.29	52665.83	52602.94	52549.42	192.31
	Difference		21.44	54.46	62.89	53.52	-
4-	**Pin**	15347.66	15340.61	15330.35	15318.62	15310.64	37.02
	Tulip	37197.29	37183.23	37143.55	37119.16	37094.87	102.42
	Pin + Tulip	52544.95	52523.84	52473.9	52437.78	52405.51	139.44
	Difference		21.11	49.94	36.12	32.27	
5	**Pin**	15198.98	15196.37	15187.95	15179.38	15167.35	31.63
	Tulip	37183.91	37176.39	37150.35	37121.6	37096.83	87.08
	Pin + Tulip	52382.89	52372.76	52338.3	52300.98	52264.18	118.71
	Difference		10.13	34.46	37.32	36.8	

Table A.6: Mass Loss [mg] for Case 2 (Without main contacts)

Sample		Control	1st	2nd	3rd	4th	Total Mass Loss
1	**Pin**	15305.04	15287.51	15234.53	15174.76	15151.74	153.3
	Tulip	37117.06	37082.1	36994.17	36907.51	36871.4	245.66
	Pin + Tulip	52422.1	52369.63	52228.7	52082.27	52023.14	398.96
	Difference		52.47	140.93	146.43	59.13	
2	**Pin**	15364.16	15360.39	15300.46	15228.49	15189.07	175.09
	Tulip	37167.7	37147.87	37045.24	36918.83	36863.08	304.62
	Pin + Tulip	52531.86	52508.26	52345.7	5217.32	52052.15	479.71
	Difference		23.6	162.56	198.38	95.17	
3	**Pin**	1523356	15229.23	15207.36	15191.02	15159.8	73.76
	Tulip	37157.13	37138.8	37099.94	37063.59	37014.35	142.78
	Pin + Tulip	52390.69	52368.03	52307.3	52254.61	52174.15	216.54
	Difference		22.66	60.73	52.69	80.46	
4-	**Pin**	15348.5	15346.58	15292.89	15233.94	15181.93	166.57
	Tulip	37430.18	37400.08	37314.94	37230.76	37151.66	278.52
	Pin + Tulip	52778.68	52746.66	52607.83	52464.7	52333.59	445.09
	Difference		32.02	138.83	143.13	131.11	
5	**Pin**	15257.29	15244.1	15171.33	15102.07	15068.07	189.22
	Tulip	37216.28	37170.26	37040.95	36940.24	36872.48	343.8
	Pin + Tulip	52473.57	52414.36	52212.28	52042.31	51940.55	533.02
	Difference		59.21	202.08	169.97	101.76	

Table A.7: Mass Loss [mg] for Case 3 (Without main contacts)

Sample		Control	1st	2nd	3rd	4th	Total Mass Loss
1	**Pin**	15205.63	15205	15194.5	15178.89	15176.28	29.35
	Tulip	37116	37105.66	37076.48	37041.86	37028.5	87.5
	Pin + Tulip	52321.63	52310.66	52270.98	52220.75	52204.78	116.85
	Difference		10.97	39.68	50.23	15.97	
2	**Pin**	15370.15	15371.02	15370.05	15357.11	15350.88	19.27
	Tulip	37200.77	37195.79	37187.59	37161.16	37143.15	57.62
	Pin + Tulip	52570.92	52566.81	52557.64	52518.27	52494.03	76.89
	Difference		4.11	9.17	39.37	24.24	
3	**Pin**	15251.87	15250.72	15245.83	15234.97	15218.35	33.52
	Tulip	37103.01	37084.6	37059.73	37029.26	37005.15	97.86
	Pin + Tulip	52354.88	52335.32	52305.56	52264.23	52223.5	131.38
	Difference		19.56	29.76	41.33	40.73	
4-	**Pin**	15283.98	15282.11	15276.44	15261.94	15252.41	31.57
	Tulip	37298.7	37286.64	37276.22	37236.59	37219.47	79.23
	Pin + Tulip	52582.68	52568.75	52552.66	52498.53	52471.88	110.8
	Difference		13.93	16.09	54.13	26.65	
5	**Pin**	15374.06	15373.94	15370.68	15350.51	15339.43	34.63
	Tulip	37191.38	37180.09	37161.45	37122.18	37099.28	92.1
	Pin + Tulip	52565.44	52554.03	52532.13	52472.69	52438.71	126.73
	Difference		11.41	21.9	59.44	33.98	

Table A.8: Mass Loss [mg] for Case 4 (Without main contacts)

Sample		Control	1st	2nd	3rd	4th	Total Mass Loss
1	**Pin**	15233.51	15237.37	15231.42	15211.42	15200.19	33.32
	Tulip	37105.2	37093.27	37079.36	37024.57	37002.37	102.89
	Pin + Tulip	52338.71	52330.64	52310.78	52235.99	52202.56	136.15
	Difference		8.07	19.86	74.79	33.43	
2	**Pin**	15298.7	15299.56	15298.91	15294.73	15287.18	11.52
	Tulip	37416	37413.14	37399.72	37385.84	37376.81	39.19
	Pin + Tulip	52714.7	52712.7	52698.63	52680.57	52663.99	50.73
	Difference		2	14.07	18.09	16.58	
3	**Pin**	15291.41	15293.5	15298.7	15297.03	15296.5	-5.09
	Tulip	37353.68	37349.91	37340.15	37323.66	37312.04	41.64
	Pin + Tulip	52645.09	52643.41	52638.85	52620.69	52608.54	36.55
	Difference		1.68	4.56	18.16	12.15	
4-	**Pin**	15299.38	15300.76	15300.54	15288.4	15287.04	12.34
	Tulip	37334.89	37330.44	37317.2	37289.94	37278.39	56.5
	Pin + Tulip	52634.27	52631.2	52617.74	52578.34	52565.43	68.84
	Difference		3.07	13.46	39.4	12.91	
5	**Pin**	15370.67	15371.42	15373.59	15374.34	15366.36	4.31
	Tulip	37480.76	37475.95	37463.21	37459.1	37439.3	41.46
	Pin + Tulip	52851.43	52847.37	52836.8	52833.44	52805.66	45.77
	Difference		4.06	10.57	3.36	27.78	

Appendix B

Measurement Results

Table B.1: Measurements from Case 1 making test (With main contacts)

Sample	Measurement	1st	2nd	3rd	4th	5th	6th	7th
1	**Arcing Time (ms)**	-	2.50	3.69	6	4.24	4.81	4.48
	Current Half-cycle (ms)	8.13	9.3	11.25	11.18	-	10.85	10.75
	Arc Current max (kA)	12.8	14.35	16.8	16.25	-	16.09	16.16
	Arc Energy (J)	-	482.18	825.67	2444.51	-	1632.9	1434.98
2	**Arcing Time (ms)**	2.58	3.39	6.12	5.13	4.22	5.33	4.96
	Current Half-cycle (ms)	10.76	9.8	12.56	9.55	9.82	9.66	11.06
	Arc Current max (kA)	18.8	15.32	17.71	14.39	14.93	14.74	16.48
	Arc Energy (J)	399.37	798.05	2003.51	1861.63	1256.61	2032.09	1495.01
3	**Arcing Time (ms)**	2.03	3	5.42	4.57	5.12	3.89	3.74
	Current Half-cycle (ms)	10.94	10.25	11.32	8.95	10.77	8.74	9.46
	Arc Current max (kA)	17	16.16	16.74	13.86	16.09	13.64	14.35
	Arc Energy (J)	292.01	695.94	2027.62	1601.25	1803.48	1103.58	927.64
4	**Arcing Time (ms)**	2.42	3.22	4.45	5.15	5.03	5.5	3.74
	Current Half-cycle (ms)	10.65	8.85	9.66	9.25	10.49	9.56	10.01
	Arc Current max (kA)	16.48	14.09	14.97	13.83	15.9	14.41	15.32
	Arc Energy (J)	344.92	796.86	1484.92	2005.16	1782.11	2518.16	887.32

Table B.2: Measurements from Case 2 making test (With main contacts)

Sample	Measurement	1st	2nd	3rd	4th	5th	6th	7th
	Arcing Time (ms)	2.69	3.4	6.17	5.87	-	5.18	6.68
1	**Current Half-cycle (ms)**	8.26	7.45	9.96	9.75	10.88	9.68	11.52
	Arc Current max (kA)	17.26	15	20.1	19.97	22.04	19.26	23.08
	Arc Energy (J)	623.85	1152	3671.79	3433.03	-	2364.91	3759.87
	Arcing Time (ms)	3.71	4.83	5.22	6.15	6.18	5.46	5.77
2	**Current Half-cycle (ms)**	10.4	10.75	10.43	10.42	10	9.97	10.94
	Arc Current max (kA)	21.85	21.65	21.14	21.07	19.91	20,07	22.11
	Arc Energy (J)	1152.21	2568.92	2605.65	3419.95	3483.11	3007.06	2671.55
	Arcing Time (ms)	4.29	4.28	6.46	4.31	6.23	5.63	
3	**Current Half-cycle (ms)**	11.63	8.02	11.09	9.18	10.09	9.87	
	Arc Current max (kA)	24.6	16.6	22.36	18.36	20.36	19.84	
	Arc Energy (J)	1248.99	1877.53	3758.39	1539.27	3694.23	3213.28	
	Arcing Time (ms)	2.83	3.04	4.57	5.94	6.37	5.63	5.33
4	**Current Half-cycle (ms)**	7.41	8.66	9.33	9.82	11	9.92	10.49
	Arc Current max (kA)	15.38	18.1	19.29	19.58	22.3	19.78	20.9
	Arc Energy (J)	860.83	817.76	2027.5	3402.61	3692.44	3201.03	2556.67
	Arcing Time (ms)	4.06	3.47	5.31	6.66	6.54	6.05	5.37
5	**Current Half-cycle (ms)**	11.42	9.41	8.95	10.6	10.9	10.27	11.11
	Arc Current max (kA)	23.91	19.52	18.31	21.14	21.72	20.9	21.98
	Arc Energy (J)	1134.75	1016.46	2812.38	4378.36	4061.94	3637.14	2472.86

Table B.3: Measurements from Case 3 making test (With main contacts)

Sample	Measurement	1st	2nd	3rd	4th	5th	6th	7th
1	**Arcing Time (ms)**	2.16	3.62	2.97	3.61	3.64	3.96	4.16
	Current Half-cycle (ms)	7.44	9.32	10.53	9.29	7.9	-	9.88
	Arc Current max (kA)	15.32	19.32	21.65	19.39	16.16	-	20.36
	Arc Energy (J)	468.39	1317.58	637.58	1325.94	1234.54	-	1587.05
2	**Arcing Time (ms)**	2.63	2.84	3.69	3.36	4.3	3.42	4.1
	Current Half-cycle (ms)	9.8	8.34	11.78	9.28	9.635	9.03	9.69
	Arc Current max (kA)	20.88	17.26	24.04	18.68	19.32	18.49	20.17
	Arc Energy (J)	488.43	803.21	926.44	993.98	1768.15	1029.74	1592.87
3	**Arcing Time (ms)**	4.05	3.52	4.82	4.34	4.48	4.43	3.99
	Current Half-cycle (ms)	10.57	8.16	10.6	10.76	9.89	10.55	9.79
	Arc Current max (kA)	22.04	16.26	21.52	21.59	19.58	21.46	20.42
	Arc Energy (J)	1470.3	1260.99	2013.72	1370.75	1805.73	1624.5	1438.25
4	**Arcing Time (ms)**	3.38	3.04	3.93	3.3	4.33	3.55	3.46
	Current Half-cycle (ms)	9.24	8.75	10.94	9	10.65	10.88	8.56
	Arc Current max (kA)	18.87	15.38	21.98	18.49	21.46	22.24	17.78
	Arc Energy (J)	1071.17	770.07	1105.03	975.68	1506.22	828.3	1202.41
5	**Arcing Time (ms)**	2.56	3.04	2.95	3.98	3.85	5.2	5.36
	Current Half-cycle (ms)	6.01	9.87	10.26	9.05	10.37	11.47	9.69
	Arc Current max (kA)	10.28	19.71	21.26	17.84	21.07	22.82	19.65
	Arc Energy (J)	503.21	678.7	617.86	1315.55	1073.12	1952	2901.99

Table B.4: Measurements from Case 4 making test (With main contacts)

Sample	Measurement	1st	2nd	3rd	4th	5th	6th	7th
1	**Arcing Time (ms)**	2.98	3.75	3.39	3.81	3.87	2.82	4.13
	Current Half-cycle (ms)	8.98	11.13	9.91	11.65	10.86	7.86	8.73
	Arc Current max (kA)	14.09	16.8	14.54	17.19	15.89	11.51	12.86
	Arc Energy (J)	612.24	856.16	680.53	777.68	804.54	595.6	1228.77
2	**Arcing Time (ms)**	3.33	3.74	3.62	3.81	3.01	4	3.47
	Current Half-cycle (ms)	10.97	9.29	9.29	11.9	10.8	11.22	9.23
	Arc Current max (kA)	16.22	13.96	13.53	17.06	16.26	16.29	13.83
	Arc Energy (J)	621.56	1082.61	916.04	745.35	499	817.02	757.81
3	**Arcing Time (ms)**	3.27	2.73	3.94	3.22	3.76	4.08	3.66
	Current Half-cycle (ms)	10.76	8.35	9.59	9.35	10.93	9.29	9.76
	Arc Current max (kA)	15.95	12.67	13.83	14.15	16.15	13.57	14.61
	Arc Energy (J)	621.43	558.7	1071.29	722.1	937.54	1104.44	875.85
4	**Arcing Time (ms)**	2.16	2.77	3.38	3.21	3.38	4.95	4.83
	Current Half-cycle (ms)	8.05	8.35	10.06	9.83	10.19	11.72	12.42
	Arc Current max (kA)	12.29	12.8	14.73	14.61	15.37	16.48	18.03
	Arc Energy (J)	354.7	571.2	688.7	655.29	797.25	1384.02	1355.28

Table B.5: Measurements from Case 1 making test (Without main contacts)

Sample	Measurement	1st	2nd	3rd	4th
1	**Arcing Time (ms)**	3.9	4.67	4.79	4.76
	Current Half-cycle (ms)	10.06	12.68	10.41	9
	Arc Current max (kA)	15.22	18.36	15.73	13.76
	Arc Energy (J)	1130.22	1076.84	1731.96	1691.11
2	**Arcing Time (ms)**	2.52	3.42	4.64	5.27
	Current Half-cycle (ms)	8.26	9.78	10.12	12.02
	Arc Current max (kA)	12.95	15.12	15.28	17.61
	Arc Energy (J)	518.02	875.44	1647.2	1543.84
3	**Arcing Time (ms)**	3.32	4.94	4.97	4.91
	Current Half-cycle (ms)	9.68	11.34	9.9	9.28
	Arc Current max (kA)	14.73	16.74	14.83	13.95
	Arc Energy (J	971.63	1611.86	1900.6	1781.2
4	**Arcing Time (ms)**	2.84	5.08	4.31	4.09
	Current Half-cycle (ms)	8.98	10.96	9.58	9.7
	Arc Current max (kA)	13.95	16.06	14.63	14.83
	Arc Energy (J)	544.26	1706.47	1396.68	1219.26
5	**Arcing Time (ms)**	2.8	4.62	4.51	4.04
	Current Half-cycle (ms)	9.5	9.12	9.42	9.91
	Arc Current max (kA)	14.66	13.63	14.41	14.89
	Arc Energy (J)	516.09	1646.49	1665.98	1112.72

Table B.6: Measurements from Case 2 making test (Without main contacts)

Sample	Measurement	1st	2nd	3rd	4th
1	**Arcing Time (ms)**	3.52	5.3	5.66	4.3
	Current Half-cycle (ms)	10.46	9.6	10.02	9.26
	Arc Current max (kA)	21.69	19.91	20.49	19.33
	Arc Energy (J)	979.39	3007.5	3127.48	1793.8
2	**Arcing Time (ms)**	2.81	5.536	6.26	4.92
	Current Half-cycle (ms)	9.82	10.56	11.78	11.1
	Arc Current max (kA)	20.69	21.66	23.63	22.82
	Arc Energy (J)	689.85	3032.26	3323.98	2086.15
3	**Arcing Time (ms)**	2.87	4.01	4.16	4.69
	Current Half-cycle (ms)	9.66	8.02	9.38	11.4
	Arc Current max (kA)	20.33	16.32	19.52	23.21
	Arc Energy (J	690.52	1702.79	1824.56	1845.96
4	**Arcing Time (ms)**	3.52	5.08	5.39	5.5
	Current Half-cycle (ms)	10.54	9.76	10.46	11.32
	Arc Current max (kA)	21.53	20.07	21.72	22.86
	Arc Energy (J)	1042.08	2574.69	2934.89	2745.82
5	**Arcing Time (ms)**	4.06	6.1	5.64	5.21
	Current Half-cycle (ms)	10.22	10.58	11.94	10.72
	Arc Current max (kA)	21.63	21.66	24.64	22.11
	Arc Energy (J)	1601.62	3873.14	2561.48	2603.11

Table B.7: Measurements from Case 3 making test (Without main contacts)

Sample	**Measurement**	**1st**	**2nd**	**3rd**	**4th**
1	**Arcing Time (ms)**	2.37	3.9	3.79	2.79
	Current Half-cycle (ms)	10.12	11.98	11.24	8.18
	Arc Current max (kA)	20.91	24.78	23.18	17.25
	Arc Energy (J)	469.54	1176.02	1094.59	712.75
2	**Arcing Time (ms)**	1.82	2.34	3.44	2.8
	Current Half-cycle (ms)	10.05	10.5	11.62	10.08
	Arc Current max (kA)	18.87	22.11	24.44	21.5
	Arc Energy (J)	348.15	467.01	857.92	796.15
3	**Arcing Time (ms)**	2.92	3.46	3.43	3.74
	Current Half-cycle (ms)	10.56	11.4	11.16	11.22
	Arc Current max (kA)	22.24	23.11	23.37	23.08
	Arc Energy (J	749.14	869.23	928.46	1172.93
4	**Arcing Time (ms)**	2.5	2.69	3.98	3.14
	Current Half-cycle (ms)	9.6	10.96	11.9	10.76
	Arc Current max (kA)	20.1	22.56	24.57	22.47
	Arc Energy (J)	603.88	566.57	1255	849.71
5	**Arcing Time (ms)**	2.52	2.88	4.1	3.45
	Current Half-cycle (ms)	11.32	9.18	11.14	10.64
	Arc Current max (kA)	23.54	18.97	22.73	22.08
	Arc Energy (J)	462.95	733.1	1250.13	966.74

Table B.8: Measurements from Case 4 making test (Without main contacts)

Sample	Measurement	1st	2nd	3rd	4th
1	**Arcing Time (ms)**	3.34	3.68	5.85	4.1
	Current Half-cycle (ms)	13.22	11.86	13.76	11.66
	Arc Current max (kA)	19.36	17.35	20.04	17.13
	Arc Energy (J)	598.91	769.73	2146.02	1056.39
2	**Arcing Time (ms)**	1.83	3.38	3.47	3.28
	Current Half-cycle (ms)	11.3	9.96	10.67	11.12
	Arc Current max (kA)	16.45	14.72	16.02	16.7
	Arc Energy (J)	214.33	859.39	807.31	673.22
3	**Arcing Time (ms)**	1.55	2.63	3.54	3.22
	Current Half-cycle (ms)	9.66	10.6	11.22	9.86
	Arc Current max (kA)	15.22	15.67	16.93	14.89
	Arc Energy (J	180.23	434.88	839.58	786.22
4	**Arcing Time (ms)**	1.74	3.12	5.04	3.08
	Current Half-cycle (ms)	9.8	10.78	13.02	9.54
	Arc Current max (kA)	15.22	16.12	18.91	14.34
	Arc Energy (J)	208.54	570.04	1749.07	783.89
5	**Arcing Time (ms)**	1.65	3.39	2.33	4.03
	Current Half-cycle (ms)	11.38	12.16	9.06	10.66
	Arc Current max (kA)	16.83	17.68	14.28	16.09
	Arc Energy (J)	155.25	615.33	440.15	1303.49

NTNU

Norwegian University of
Science and Technology